Ital. J. Geosci., Vol. 137 (2018), pp. 00, 15 figs., 6 tabs. (https://doi.org/:10.3301/IJG.2018.04)
© *Società Geologica Italiana, Roma 2018*

Geochemical, mineral-petrographic and physical-mechanical characterization of stones and mortars from the Romanesque Saccargia Basilica (Sardinia, Italy) to define their origin and alteration

Stefano Columbu ([a*]), Marcella Palomba ([b]), Fabio Sitzia ([a]) & Miriam R. Murgia ([a])

ABSTRACT

This paper aims to study the geomaterials of the most important Romanesque-style monument of Sardinia, the *Santissima Trinità di Saccargia* Basilica (Codrongianos, north Sardinia). The monument was built up on ruins of a pre-existing monastery, and completed in 1116 A.D. Over time, the aspect of the monument is quite changed due to two series of restoration works. The stone materials consist of both grey-black basalts and whitish limestones and marls, intentionally used to give a bichromy effect of the construction. The volcanic rocks belong to the Miocene-Pleistocene volcanic Sardinian activity, while limestones and marls belong to the sedimentary marine Miocene Formation of Meilogu (Logudoro).

To define both the origin and the alteration processes of materials, geochemical, petrographic and physical-mechanical investigations of volcanic and sedimentary rocks were carried out on samples collected from monument and possible source outcrops.

The integrated chemical (ICP-MS) and petrographic data allowed to ascertain the sourcing sites of raw materials. Moreover, physical-mechanical tests along with X-Ray Diffraction (XRPD) analysis, highlighted the main weathering processes responsible of the chemical-physical alteration affecting the geomaterials, and the newly-formed mineral phases formed on stone surface.

Key words: *Medieval monuments, ICP-MS chemical analysis, Archaeometry, Volcanic rock, Limestone and marl.*

INTRODUCTION AND AIMS

The Santissima Trinità of Saccargia Basilica (Figs. 1, 2) is a Romanesque-style monument located in the municipality of Codrongianos, Sassari province (north Sardinia, Italy; Fig. 3). It was completed in 1116 A.D. and consecrated on October 5 of that year. Originally, as nowadays, the structure forms a *Tau* cross drawing, with NW-SE orientation axis, and a transept overlooked by three apses faced toward SE (Fig. 2a). The apses have different dimension, where the central (Figs. 1b, 2b) is the highest and wide. A portico is placed in front of the façade (Figs. 2a, 1d, 1e), while the bell tower and the sacristy, connected with the nave and the head of the transept, are located in the northern section. Ruins of a pre-existing monastery's cloister occur in the southern sector of the site (Fig. 2a). Several evidences testify that the monument was built up into two phases: during the first phase, much of the transept and the covered nave, with wooden roof, were carried out. The walls were built up using ashlars of whitish sedimentary (*i.e.* limestones, marls) and greyish volcanic lithologies (*i.e.* basaltic rocks) in alternating rows as *"Opera Bicroma"* (the bichromy, Fig. 1c, was very appreciated and frequently used in medieval period), according to the technique of the Pisan-Pistoian workers, operating in *Giudicato Turritano* at the end of XI century (Sechi, 1992). The second phase of building correspond to the raising of the nave, which extends westwards, and the present façade (Fig. 1h), partially demolished and then rebuilt up in early twentieth century (Coroneo, 1993; Serra, 1988).

Over time, the monument was submitted to expansion and restoration works. From 1118 to 1120, architects and craftsmen of Pisan school carried out the following interventions: expansion of the building such as extension of the main nav raising of the walls and a new façade, and the construction of the bell tower (Figs. 1a, 1b, 2c). The portico before the façade maybe was added later, at the completion of the basilica, and its construction is attributed to the Tuscany workforce (Coroneo, 1993).

In the late nineteenth century, a first restoration phase consisted in the removal of the inner plasters. A later restoration, carried out between 1903 and 1906, consisting in the main prospect's demolition and some interventions in the highest parts of bell tower, was supervised by at the time superintendence chief Filippo Vivanet. During this intervention, Vivanet refers about the degradation of the limestone ashlars. Furthermore, he made reference to the replacement of the columns in the bell tower's mullioned windows with granite columns coming from Monti (Gallura province, Sardinia), as well as the rebuilding of some walls "made in previous patches" (Vivanet, 1902).

Scano (1908) also mentions the intervention work, between 1903 and 1906 (which he himself did, under the supervision of Filippo Vivanet), carried out on the columns of the portico. In earlier times (not better defined), the columns were reinforced with limestone and volcanic ashlars, in order to create, around the pillar, a quadrangular section able to better support the load, since the limestone blocks, excessively friable, proved to be little suitable for the purpose (Scano, 1908).

To study and understand the complexity of similar monuments, the investigations on the geomaterials (*i.e.*

([a]) Dipartimento di Scienze Chimiche e Geologiche - Università di Cagliari, Via Trentino 51, 09127 Cagliari, Italy.
([b]) Istituto di Scienze dell'Atmosfera e del Clima (ISAC) del C.N.R., Unità Operativa di Supporto (UOS) di Cagliari, c/o Dipartimento di Fisica, Università di Cagliari, Strada Provinciale Monserrato Sestu Km. 0,700, 09042 Cagliari, Italy.
Corresponding author e-mail: columbus@unica.it.

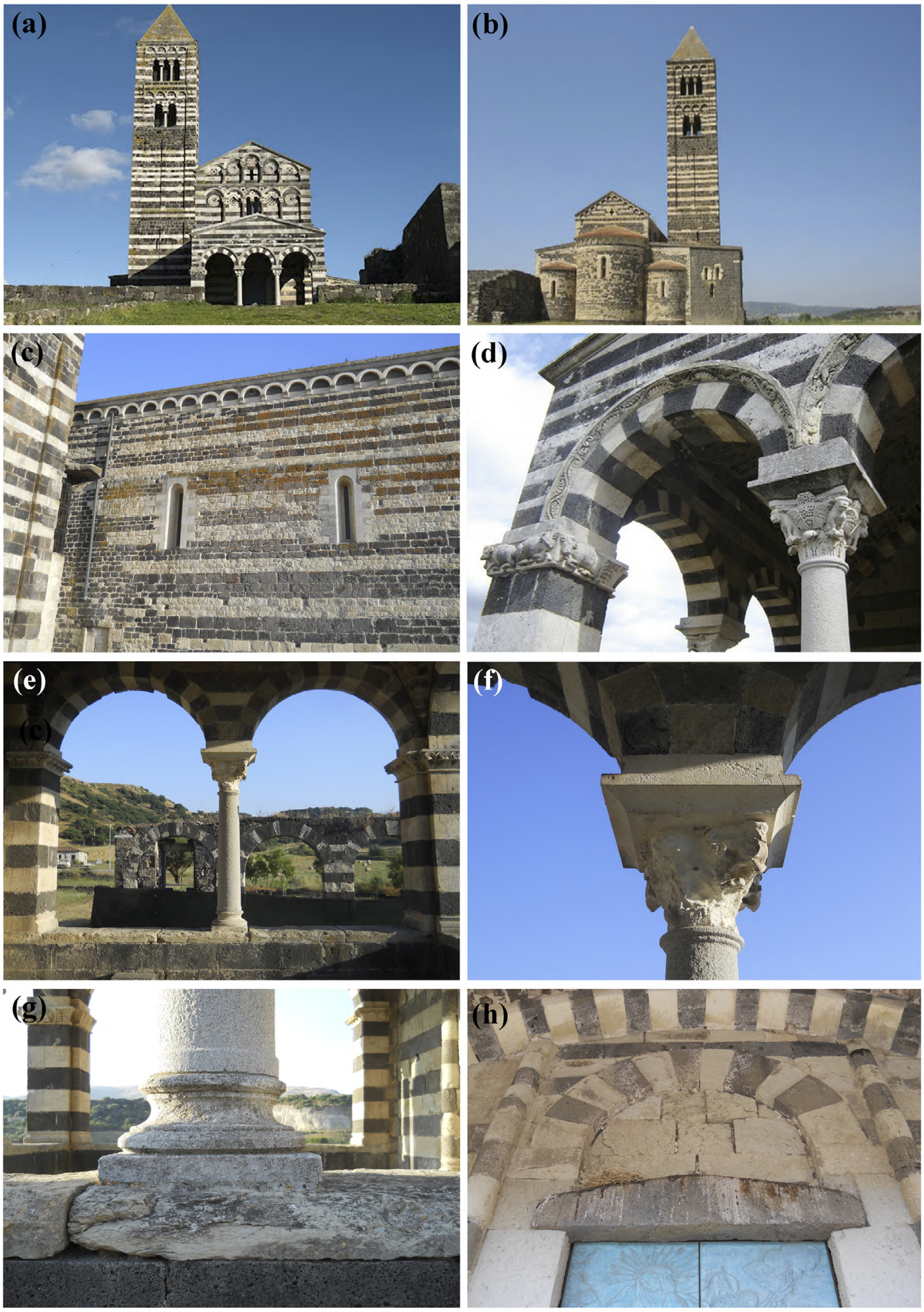

Fig. 1 - The Saccargia Basilica: (a) monument facade; (b) three apses with different height; (c) "Opera Bicroma" rock rows; (d) facade porch (north-ovest view); (e) façade porch (view toward the perimeter wall of outside courtyard); (f) limestone column capitals; (g) limestone column basement; (h) current façade.

stones and ancient mortars) should be addressed in a multidisciplinary way (Antonelli *et alii,* 2014a, 2014b; Bertorino *et alii,* 2002; Columbu, 2017, 2018; Columbu *et alii,* 2014, 2015a, 2015b, 2016, 2017a, 2017b, 2018a, 2018b; Columbu & Garau, 2017; Columbu & Verdiani, 2014; Lezzerini *et alii,* 2016, 2018; Miriello *et alii,* 2015; Verdiani & Columbu, 2010). All scientific and technical activities, related both to architectural, archaeological and geological topics, should synergistically focus to achieve the common objective for better understanding the cultural significance of a monumental building as part of its historical, artistic and political context. From this standpoint, the applied petrography was recently played an important role in archaeometric studies of Culture Heritage, providing significant information about geochemical and petro-physical features of geomaterials used in the construction. The knowledge and the base skills of the above-mentioned disciplines are fundamental to address specific issues or

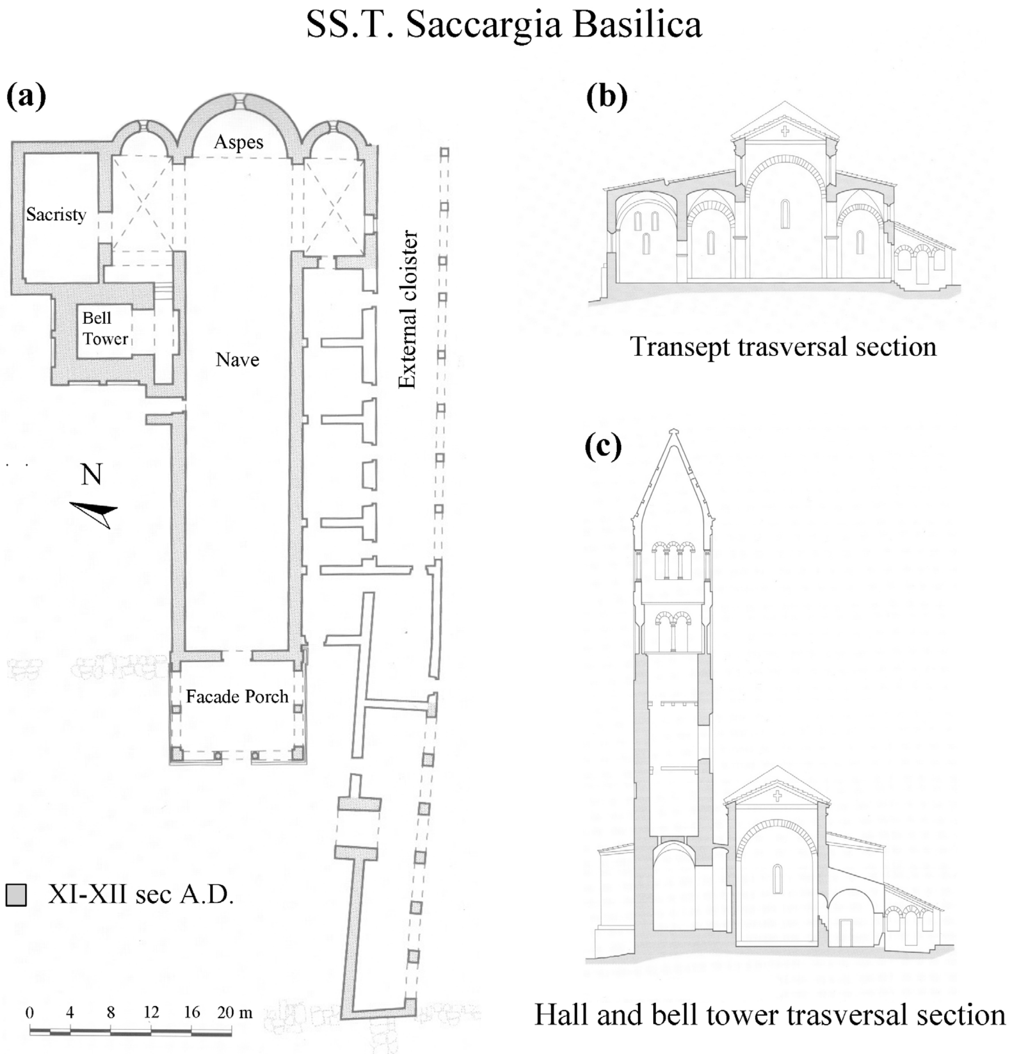

Fig. 2 - The Saccargia Basilica: (a) plan; (b) transept transversal section; (c) hall and bell tower transversal section.

historical archaeology (*e.g.* origin and the trade routes of geomaterials, construction technology, patterns of use, workability etc.) or conservation problems (*e.g.* analysis of weathering decay, techniques of conservation, protection and restoration of these monuments).

The petrographic study, integrated with mineral and chemical analyses, of the monument materials and the quarry stones provides meaningful data for the petrographic classification of the rocks. These studies can also provide information, by comparison, about geographic/geological features of the country of provenance allowing, sometimes, to exactly localizing the ancient quarries of origin.

Furthermore, the analysis of some physical properties of geomaterials (density, porosity, water absorption, saturation index, mechanical strength, etc.) allows checking the technical features of the stone for monument's construction. Several studies focused on the stone materials widely used in historic periods in Sardinia, from Neolitic (Bertorino *et alii,* 2002; Columbu *et alii,* 2013) to Punic-Roman (Antonelli *et alii,* 2014; Columbu & Garau, 2017; Melis & Columbu, 2000), to middle ages (Columbu & Verdiani, 2014; Coroneo & Columbu, 2010; Columbu *et alii,* 2014; Columbu, 2017; Gizzi, 2007; Macciotta *et alii,* 2001) and recent time (Columbu *et alii,* 2011).

There are no recent specific works on the geomaterials used for the Romanesque Saccargia Basilica. For this reason, the present paper intend to give a contribute to knowledge of the monument and the construction materials in order to define: 1) the origin of volcanic and sedimentary rocks sampled from the monument and in the surrounding field, by integrating petrographic and chemical data; 2) the alteration processes affecting the stones, by mineralogical studies carried out to determine the newly-formed mineral associations formed on the exposed stone surfaces as well as the physical-mechanical properties of the samples collected from the monument and on field; 3) the composition of the original ancient bedding mortars, their typical alterations, and the binder/aggregate mixtures to understand the construction technologies used in medieval times.

GEOLOGICAL CONTEXT

The Saccargia Basilica is situated in the Codrongianos-Florinas area (Fig. 4), sub-region of *Meilogu* (Logudoro,

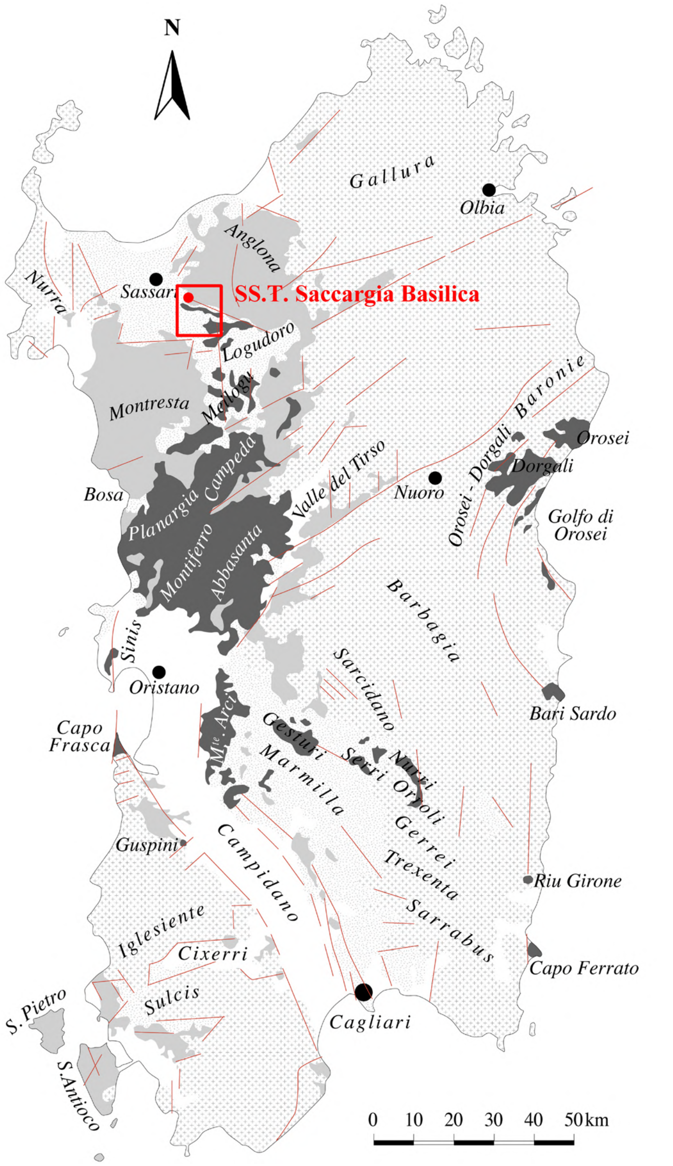

Fig. 3 - Geological map of Sardinia with geographical localisation of the Saccargia Basilica.

northwestern Sardinia). The area is placed along the Sardinian Oligo-Miocene rift, a large tectonic pit, which structure crossing Sardinia (Advokaat *et alii*, 2014; Cherchi & Montadert, 1982a, 1982b; Coulon, 1977; Dostal *et alii*, 1982), where, besides also other areas of Sardinia, the Sardinian igneous activity occurred. It is generally related to a N-NW deeping subduction of the Ionian oceanic lithosphere which developed (probably since Middle-Late Eocene) beneath the Paleo-European-Iberian continental margin which led, during the Oligocene, to the formation of the rift between Sardinia and Provence (Beccaluva *et alii*, 1989, 2011; Burrus, 1984; Cherchi *et alii*, 2008). Cenozoic volcanism is subdivided in two main following phases (often overlapped in space), different in time and magmatic affinity (Beccaluva *et alii*, 1989, 2005a, 2005b, 2011; Lustrino *et alii*, 2011): 1) orogenic magmatic activity (including tholeiitic, calcalkaline, shoshonitic and ultrapotassic products) developed mostly during Late Eocene–Miocene times (~ 38–15 Ma), where major and trace element indicators, as well as Sr–Nd–Pb–Hf–Os–O isotope, indicate complex petrogenetic processes including subduction-related metasomatism, variable degrees of crustal contamination at shallow depths, fractional crystallization and basic rock partial melting (Lustrino *et alii*, 2013); 2) anorogenic magmatism (with tholeiitic to Na-alkaline products) occurring during Late Miocene–Quaternary times (~ 12 to ~ 0.1 Ma), geochemically unrelated to active or recent subduction processes (*e.g.*, Lustrino *et alii*, 2007, 2009, 2011). The orogenic and anorogenic magmatic phases are well-constrained in space and time and are correlated with regional tectonics (Beccaluva *et alii*, 2011). Geophysical data indicate that flattened relics of the Cenozoic Apennine–Maghrebian subduction still exist below Sardinia and the Betic–Calatrava districts in Southern Spain (Piromallo & Morelli, 2003; Spakman, 1990).

In Meilogu area Oligo-Miocene products (pyroclastites, acid and andesitic lavas; thematisms 18, 19b,c in Fig. 4) and Plio-Pleistocene volcanic rocks (thematisms 18a, 4b in Fig. 4) crop out. These latter, which were used as construction materials for the Saccargia Basilica, belong to the Late Miocene-Quaternary anorogenic magmatism. Moreover, sedimentary formations crop out in Meilogu area, covering a time period ranging from Miocene to Holocene (Fig. 4).

Sardinian anorogenic magmatism

Geochemical and petrological characteristics

The Late Miocene-Quaternary anorogenic magmatism activity is associated with the extensional tectonics, probably linked to the collapse of the Tyrrhenian area. This magmatism occurred in back-arc settings (*e.g.* Sardinia and some volcanoes in the southern Tyrrhenian Sea) and on the margin of the African foreland (*i.e.* Iblei, Etna, Sicily Channel), Peccerillo & Frezzotti, 2015.

Radiogenic isotope data show a wide compositional range, mostly with EM-I (Enriched Mantle-I; Gasperini *et alii*, 2000, 2002; Lustrino *et alii*, 2013; Peccerillo & Frezzotti, 2015) characteristics for Sardinian magmas, and only a subordinate HIMU-like signature (Beccaluva *et alii*, 2005b, 2011), in southern area of the island (Lustrino *et alii*, 2000). By Sr–Nd–Pb–Hf–Os isotopic data, it is possible to subdivide these rocks (according to Lustrino *et alii*, 2013, 2017) in: 1) radiogenic Pb volcanics (inlcuding the oldest and very rare products, ~ 12–4.4 Ma) occurring only in the southern sectors of Sardinia; 2) unradiogenic Pb volcanics, including the rocks emplaced of central and northern sectors (~ 4.8–0.1 Ma).

Geochemical and petrological features of Sardinian anorogenic volcanism and associated mantle xenoliths indicate that primary magmas - from tholeiites through alkali basalts to basanites - were generated by decreasing melting degrees of progressively deeper lithospheric mantle sources at depths between ca. 30 to 100 km (Beccaluva *et alii*, 2011).

The magmatic activity started at 11.8 Ma in Isola del Toro (SW Sardinia) with an abrupt change in terms of chemistry, petrography and volcanological facies compared with the older igneous activity (Lustrino *et alii*, 2007, 2009). Then, after a quiescence of ~ 5 Ma, the volcanic activity mainly developed in the time span ~ 6 to < 0.1 Ma (Beccaluva *et alii*, 1985a, 1989; Lustrino *et*

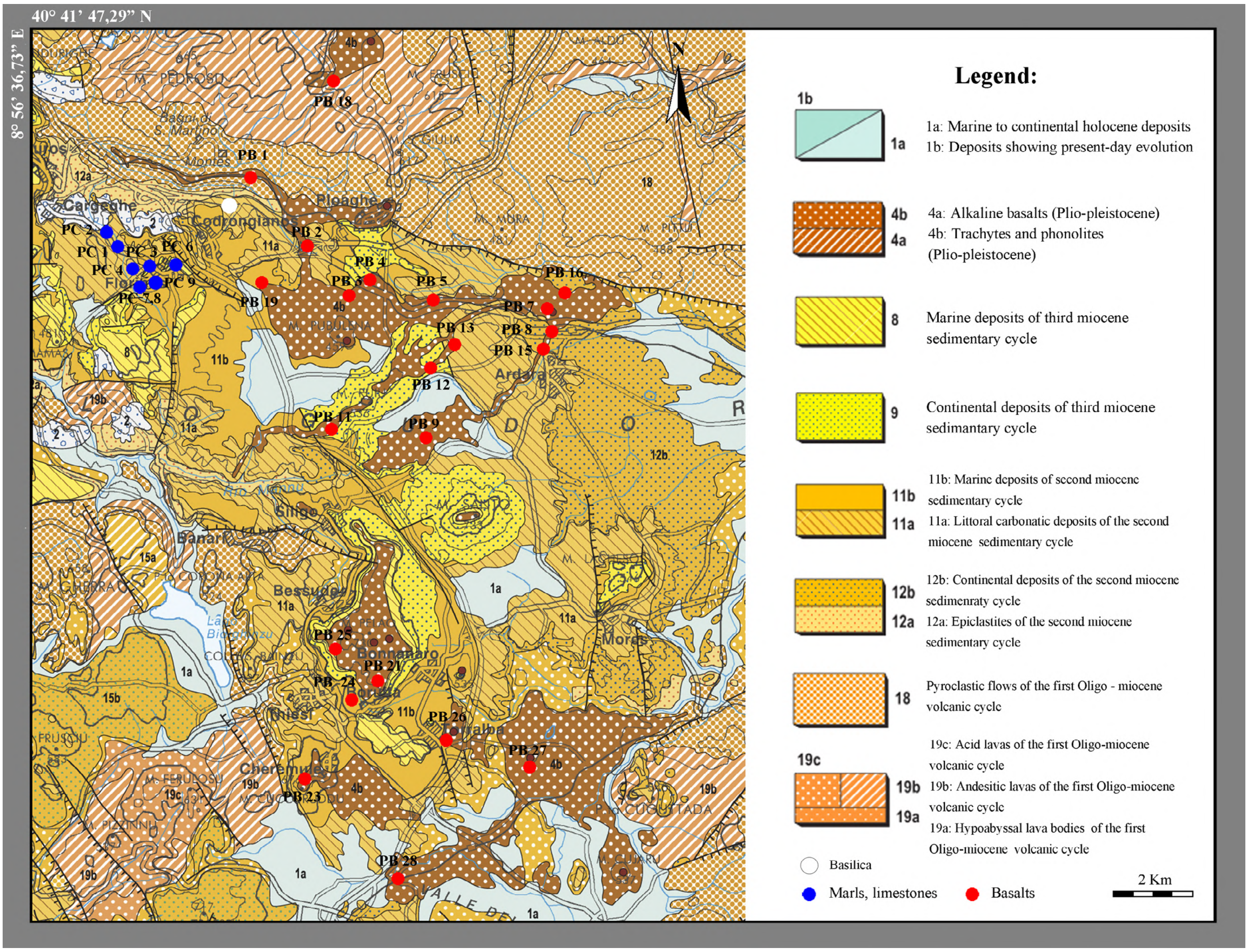

Fig. 4 - Geological maps of investigated area from Logudoro sector with sampling points of marls, limestones and basalts (from Carmigniani *et alii*, 2015, modified).

alii, 2007; Peccerillo & Frezzotti, 2015), starting from the southern sector of Sardinia only (Capo Ferrato, Rio Girone and Guspini; Lustrino *et alii*, 2000, 2007) and continuing in other Sardinian areas. This volcanism overall produced mafic to silicic subalkaline, transitional to Na-alkaline rocks (sometimes with a K-affinity; Peccerillo & Frezzotti, 2015). The major and, partially, trace element content of these rocks roughly resemble magmas emplaced in within-plate tectonic settings (Lustrino *et alii*, 2013). The volcanic rocks generally have: lower CaO and higher K_2O and K_2O/Na_2O than equivalent rocks from Sicily (*e.g.* Beccaluva *et alii*, 2011; Lustrino *et alii*, 2013) and a rather smooth upward-convex OIB-type pattern, sometimes with relative depletion in Cs, Rb and K (Peccerillo & Frezzotti, 2015).

During early Pliocene to Quaternary in age (~ 6-0.1 Ma), the Na-alkaline basaltic volcanic activity, occurring in eastern Sardinia, offshore areas, as well as in the NW-SE striking Campidano graben (south-western Sardinia), was essentially of fissural type (mainly as basaltic plateaux), due to an extensional regimen that has reactivated faults of various orientations (Beccaluva *et alii*, 1985).

The erupted products are mainly alkaline basalts, with minor subalkaline basalts, and differentiated products along different areas of the island, covering an area of ~ 2000 km^2 (Beccaluva *et alii*, 2011).

The Capo Ferrato products (5.3-4.9 Ma; Beccaluva *et alii*, 1985) had a transitional character (the following volcanic products had an alkaline and subalkaline character, while the latter products (Logudoro < 0.5 Ma) had a purely sodic alkaline character. Volcanic effusions are concentrated in particular areas such as Montiferro complexes (3.9 to 1.7 Ma), Mount Arci complex (3.8-2.8 Ma), Orosei Gulf (3.9-2.1 Ma), plateaux of Planargia-Campeda and Abbasanta (3.8-1.7 Ma), plateaux (Giare) comprised between Marmilla and Sarcidano (3.8-1.7 Ma) and finally, more recently, Logudoro (2.9-0.1 Ma) in the northern part of Sardinia (Beccaluva *et alii*, 1985; Peccerillo & Frezzotti, 2015).

Plio-Pleistocenic volcanic rocks of Sardinia include many types of xenoliths, of both crustal and mantle origin. Crustal xenoliths are largely diffused in the rocks with alkaline and subalkaline affinity. The mantle xenoliths can be only found in the sodic alkaline series, in particular in the following areas: Orosei-Dorgali, Montiferro, Logudoro, Rio Girone, Central Sardinia and, more rarely, in the Mount Arci area (Beccaluva *et alii,* 2001, 2010; Lustrino *et alii*, 2004).

The three major volcanic evolutionary series were defined based on different patterns of major and trace elements (Peccerillo, 2005; Peccerillo & Frezzotti, 2015): 1) a strongly Na-alkaline serie, strongly undersaturated in silica, ranges from basanite-tephrite to phonolite in composition, with some of the most evolved rocks reaching a peralkaline composition (it is best represented in the volcanic complex of Montiferru, western Sardinia); 2) a moderate alkaline/transitional serie, undersaturated silica in a non-critical way, with a Na- to mildly K-alkaline affinity, ranging from trachy-basalt to trachyte (with outcrops in several areas of Sardinia,); 3) a subalkaline silica saturated to silica-oversatured serie (basalt - basaltic andesite - dacite - trachyte - rhyolite) with tholeiitic affinity (it occurs at Mount Arci).

The alkaline mafic volcanics are more enriched in incompatible trace elements and less enriched in silica with respect to oversaturated tholeiitic rocks with similar MgO amounts. REE show smooth and fractionated patterns (Peccerillo, 2005).

According to Lustrino *et alii* (2004a), at radiogenic isotopic variations corrispond systematic modifications of trace element in Sardinian Plio-Quaternary volcanics; *i.e*., a negative correlation between Ba/Nb *vs*. Ce/Pb ratios was highlighted.

Logudoro volcanism

The Logudoro area represents the northernmost activity and it contains the youngest rocks (2.9-0.1 Ma) of Sardinian Plio-Quaternary anorogenic volcanism. The products associated to the intense volcanic activity occurred in Logudoro (about 500 km^2) were later placed simultaneously to the erosion of the basaltic platforms of Planargia, Planu Mannu, Pranu Murtas and Campeda (Beccaluva *et alii*, 1975). Logudoro volcanism manifested by the effusion of basic lavas with significant changes in composition, extending up to a few kilometres from the mostly emission centres, also generating an explosive activity causing several volcanic cones (Mt. Cujaru, Ittireddu; Mt. Austidu, Cheremule; Mt. Meddaris, Ploaghe).

This volcanism develops on three main tectonic lines, approximately having N-S, NE-SW and NW-SE directions. Most emission centers occur in the area between Mt. Pelao and Mt. Austidu, as well as near the inhabited area of Giave.

The Plio-Quaternary volcanism from northern Sardinia (including the Logudoro sector), as well as the central sector of the island, has a peculiar unradiogenic Pb–Nd isotopic composition, that is unique in Europe, and resembles EM-1 OIB-type rocks (Peccerillo & Frezzotti, 2015). According to Gasperini *et alii* (2000), the unradiogenic Pb-isotope signatures of Logudoro basalts are accompanied by high Ba/La and Eu/Eu and Sr/Eu values, and relatively higher Ce/Pb values and lower Nb/U values in comparison with uncontaminated oceanic basalts.

The Sardinian anorogenic magmas generally show low LILE/HFSE ratios, resembling intraplate igneous rocks occurring in several places in Europe (Peccerillo & Frezzotti, 2015). REE patterns and mantle-normalised incompatible element patterns of mafic rocks show a slightly upward convexity with moderate enrichment in Nb and positive marked spikes of Ba and Pb (Peccerillo, 2005).

The volcanism manifests in the Logudoro area with a mostly alkaline character with a sodic to mildly potassic affinities, while the subalkaline rocks occur in minor amounts (Peccerillo, 2005). Rock types include basanites, trachybasalts, basaltic trachyandesites and basaltic andesites (Beccaluva *et alii*, 1976, 1977, 1985a; Savelli, 1988; Gasperini *et alii*, 2000). On the contrary in Campeda, Planargia and Planu Mannu platforms, located southward and eastward, subalkaline basaltic lavas and, to a lesser extent, weakly alkaline and transitional ones are major (Beccaluva *et alii*, 1975). According to Beccaluva *et alii* (1975, 1976) and further unpublished data, some chemical elements show a wide variation as function of alkalinity degree. On the whole, from subalkaline to alkaline basaltic lavas, there are a particularly marked increase in P, Ti, Sr and Nb and a decrease in Y/Nb, K/Rb, Na_2O/K_2O ratios, similarly to the behaviour recognized at regional scale concerning several Plio-Quaternary basic volcanites in Sardinia.

The Logudoro volcanics show intermediate values of Ba/Nb and Ce/Pb ratios with respect to the volcanics of other Sardinia sectors (Peccerillo, 2005).

Sedimentary rocks of Logudoro

These rocks belong to the Sardinian Miocene marine sedimentary sequence, represented by at least 1000 meters of siliciclastic and mixed carbonate-silicoclastic sediments and with associated pyroclastic and epiclastic products of coastal environment. These formations are interposed between continental and /or transitional deposits connected with regressive phases and constituted by conglomerates, sandstones and clays at times carbonates of river environments, deltices and lakes. The first sedimentary phase is represented by marine and continental sediments, conglomerates and silty clays affecting a wide area of central-southern Sardinia. The second sedimentary phase is mainly represented by sandy and carbonatic sediments that crops out in the northern area of Sardinia. The third sedimentary phase mainly affected areas of central-west Sardinia and area of Cagliari; however, limestone formations belonging to this phase are also present in the area of northern Sardinia (Assorgia *et alii,* 1997).

The rocks crop out in Florinas area (northern Sardinia) belong to the second and third sedimentary marine Miocene phases (Fig. 4).

Above the volcanic substrates, at least five lithostratigraphic sedimentary units, closest to the monument, were recognized and described in their stratigraphic relations by Mazzei & Oggiano (1995): Lower sands *(Si)*, Lower limestones *(Ci)*, marly-arenaceous unit *(Uma)*, Upper sands *(Ss)*, all represented with thematisms 11b, 11a in Fig. 4, and Upper limestones *(Cs)*, thematism 8 in Fig. 4.

The second Miocene marine transgression phase (Lower-Middle Miocene) occurred in the area accumulating the Lower sands and Lower limestone. Furthermore, in that time began the bathymetric deepening of the area that favoured the sedimentation of the Lower sands *(Si)*, Lower limestones *(Ci)* and the marly-arenaceous unit *(Uma)*.

The second cycle is characterized by a bathymetry surely greater than the third (though not more than 100 m deep), which can be associated to the N-NO subsidence of the pit (Mazzei & Oggiano, 1995).

The third sedimentary cycle (Upper Miocene), represented by the Upper limestone *(Cs),* is characterized by low bathymetric; the influences of eustatic character, within this cycle, cannot be excluded. The *Cs* unit, due to mixed deposition environments, is attributed to Tortonian-Lower Messinian period. The Upper limestone *(Cs)*, superimposed on marls *(Uma)* and sand units *(Si, Ss),* is strongly related to the morphological and structural pattern outlined before the same third marine transgression. This unit has proved difficult to date; its attribution to the lower Messinian, at the moment only hypothetical, would however explain some aspects that affect it, such as slip structures, accumulations of «algal balls», «crumpled beds» and sin-sedimentary breccias present in the area (Mazzei & Oggiano, 1990).

MATERIAL AND METHODS

Sampling

Sampling of the monument materials was made according to Recommendations Nor.Ma.L. 3/80 and in agreement with the Superintendence of Cultural Heritage, which regulated the number of samples collected for laboratory destructive analysis. Sampling was carried out according to the Nor.Ma.L. 3/80 recommendations concerning: material *in situ*, material no longer operates and no longer recoverable in artifact and quarry outcrops. Sampling (Fig. 4) is then associated to a "sample log card" (according to a Nor.Ma.L. 2/80 storage document). Tables 1, 2 show sampled points, their height on monument, with respect to the ground level around the Basilica, and the altitude point (MASL) together with the geographical coordinates of the sites, in case of field outcrops.

TABLE 1

Macroscopic description and data of samples taken from the Saccargia Basilica (Codrongianos) of volcanic rocks, sedimentary rocks (limestones and marls) and ancient mortars and plasters (*rinzaffo* and *arriccio* layers). Abbreviations: B = binder; A = aggregate; ∅ = frequently aggregate diameter range.

Sample	Lithology	Sampling height (cm)	Macroscopic features	CIELAB colouring
STS 14	Volcanic rocks	5	Massive facies, pores ∅ < 0.5 mm	62*0*11
STS 20		30	Massive facies, pores ∅ < 0.6 mm	62*0*11
STS 15		40	Vacuolar facies, pores ∅ < 1 - 1.5 mm	46*-1*2
STS 18		40	Vacuolar facies, pores ∅ < 1 - 2 mm	74*-1*-4
STS 22		40	Vacuolar facies, pores ∅ < 1 - 1.5 mm	84*-1*-4
STS 24		20	Vacuolar facies, pores ∅ < 1 - 1.5 mm	74*-1*-4
STS 25		0	Vacuolar facies, pores ∅ < 1 - 1.2 mm	74*-1*-4
STS 28		40	Vacuolar facies, pores ∅ < 1 - 1.9 mm	58*-2*-3
STS 17	Sedimentary rocks	35	Altered arenaceous marl, 5% vol. bioclasts, bioturbation	99* -3*-8
STS 13		35	Altered arenaceous marl, 10% vol. bioclasts	77*-1*1
STS 21		70	Massive arenaceous marl, 5% vol. bioclasts	99* -3*-8
STS 26		120	Massive arenaceous marl, 7% vol. bioclasts	89*1*11
STS 29		190	Massive arenaceous marl, 4% vol. bioclasts	89*1*11
STS 19		180	Detritic organogenic limestones, 60% vol. bioclasts	47*1*6
STS 37		20	Arenaceous limestones, 3% vol. bioclasts	70*1*-6
STS 32	Mortars	60	Aggregate with ∅ = 0.1 - 6 mm, B/A ratio ~ 0.35-0.5	84*0*-1
STS 33		60		84*0*-1
STS 36		85		84*0*-3
STS 1	Plasters (*rinzaffo layer*)	40	Aggregate with ∅ = 0.1 - 3 mm, B/A ratio ~ 2	90*0*-3
STS 5		30		
STS 6		30		
STS 3	Plaster (*arriccio layer*)	20	Aggregate very fine, with ∅ < 1.5 mm, B/A ratio > 3	67*0*-3

TABLE 2

Samples taken from the outcrops with description of the sampling points reported in Fig. 4. Volcanic rocks are classified according to Le Maitre *et alii* (2002) diagram. Limestones and marls are classified trough optical polarized microscopy.

Sample	Lithology classification	Sampling coordinates (deg., min., sec.)	Altitude (MASL)	Sampling municipality and locality	Distance from Basilica (km)
PB 1	Basaltic trachy-andesite	40° 40' 34,58"N 8° 41' 17,55"E	245	Codrongianos, P. De Coloru	0.5
PB 2		40° 39' 26,86"N 8° 43' 51,61"E	426	Ploaghe, San Michele	3.8
PB 3		40° 38' 23,92"N 8° 42' 56,00"E	366	Ploaghe, Su Trialzu	3.8
PB 4		40° 38' 41,27"N 8° 44' 30,43"E	371	Ploaghe, Monte Meddaris	5.3
PB 5		40° 38' 39,81"N 8° 43' 38,71"E	349	Ploaghe, Planu e Filighe	7.2
PB 7		40° 37' 59,11"N 8° 48' 41,18"E	261	Ardara, Monte Frisciu	11.1
PB 8		40° 37' 31,75"N 8° 49' 1,55"E	256	Ardara, Planu su Achileddu	11.9
PB 9		40° 35' 57,85"N 8° 45' 39,35"E	333	Siligo, Planu Coveccadu	10
PB 11		40° 36' 30,81"N 8° 43' 52,11"E	402	Siligo, Scala Plogaese	7.8
PB 12		40° 37' 17,61"N 8° 45' 49,73"E	376	Siligo, Scala Torta	8.3
PB 13		40° 37' 32,37"N 8° 46' 12,45"E	355	Siligo, Scala Torta	8.5
PB 15		40° 37' 51,58"N 8° 48' 32,93"E	275	Ardara, C. Codina Preideros	11
PB 16		40° 38' 40,07"N 8° 48' 57,31"E	277	Ardara, Pedralada	11.1
PB 18		40° 41' 51,26"N 8° 43' 49,39"E	484	Ploaghe, Bilione	4.5
PB 19		40° 38' 39,90"N 8° 41' 58,03"E	340	Codrongianos, Charchidana	3.1
PB 21		40° 31' 32,66"N 8° 44' 30,15"E	571	Borutta, Cannarzu	16.7
PB 23		40° 30' 1,62"N 8° 43' 31,34"E	544	Cheremule, Perdas	19.2
PB 24	Trachy-basalt	40° 31' 41,17"N 8° 44' 31,07"E	530	Borutta, Costaccones	16.5
PB 25		40° 31' 57,97"N 8° 43' 47,21"E	571	Thiesi, Sas Funtaneddas	15.7
PB 26	Basaltic trachy-andesite	40° 30' 50,99"N 8° 46' 11,30"E	453	Torralba, Monte Oes	18.7
PB 27	Basaltic-andesite	40° 30' 32,32"N 8° 47' 51,99"E	377	Torralba, Monte Austidu	20.2
PB 28	Basaltic trachy-andesite	40° 28' 11,48"N 8° 45' 14,01"E	480	Giave, Monte Annaru	23
PC 1	Detritic organogenic limestone	40° 39' 33,66"N 8° 38' 14,50"E	356	Florinas, Funtana Fritta	4.5
PC 2		40° 39' 44,94"N 8° 38' 4,50"E	347	Florinas, Funtana Fritta	4.7
PC 3	Arenaceous marl	40° 38' 53,21"N 8° 38' 49,56"E	396	Florinas, Pedra Ladra	4.4
PC 4		40° 38' 41,66"N 8° 38' 49,98"E	376	Florinas, Pedra Ladra	4.6
PC 5	Detritic organogenic limestone	40° 38' 44,14"N 8° 39' 17,61"E	444	Florinas, Monte Sorighe	4.1
PC 6		40° 38' 59,36"N 8° 40' 8,86"E	435	Florinas, Monte C. e Cheia	2.9
PC 7		40° 38' 44,76"N 8° 39' 18.46"E	446	Florinas, Monte Sorighe	4.4
PC 8		40° 38' 45,17"N 8° 39' 18,80"E	445	Florinas, Monte Sorighe	4.3
PC 9	Arenaceous marl	40° 38' 33.38"N 8° 39' 17.02"E	390	Florinas, Sud M. Sorighe	4.6

Sampling on the monument (Table 1; Fig. 2a) consists of 22 samples: 8 volcanic rocks (STS: 14, 15, 18, 20, 22, 24, 25, 28), 7 marl and limestone rocks (STS: 13, 17, 19, 21, 26, 29, 37), 3 original mortars (bedding of stone ashlars, STS: 32, 33, 36) and 4 plasters (STS: 1, 3, 5, 6).

From the local geological outcrops (Table 2, Fig. 4), in a radius of about 20 km away from the monument, further 22 volcanic samples were collected (PB: 1-5, 7-9, 11-13, 15, 16, 18, 19, 21, 23-28) outcropping in the Meilogu sub-region (Logudoro, north Sardinia), and 9 marls and limestone rocks (PC: 1-9).

Petrographic, chemical, mineral and petro-physical methods

Petrographic determinations of mineralogical composition were carried out on polished thin sections by optical polarised microscope Leitz Wetzlar.

Chemical analyses on the volcanic samples from the monument and outcrops were performed at the laboratory of ALS Minerals (Siviglia, Spain) by Inductively Coupled Plasma Atomic Emission Spectroscopy (ICP-AES, by lithium borate fusion) for major elements and by Inductively Coupled Plasma Mass Spectrometry (ICP-MS) for trace elements.

Classification of the volcanic rocks and relative nomenclature was carried out according to Le Maitre *et alii* (2002).

X-Ray Powder Diffraction technique (XRPD) was applied to the sampled building materials, belonging to both the rocks and mortars, for determining the qualitative/semi-quantitative mineralogical composition of powdered samples. The XRPD data were acquired using an experimental package Rigaku Miniflex II, equipped with auto-sampler, goniometer and monochromator systems, using the Cu kα radiation, X-Ray tube at 30 kV and 30 mA, Ni filter, scanning 4-60° 2ϑ, step sampling 0.02° 2ϑ, acquisition rate 1° 2ϑ/min. Data of some afterwards selected samples, for semi-quantitative analysis, were acquired according to the following instrumental conditions: Cukα radiation, 30 kV, 30 mA, Ni filter, sampling step 0.01° 2ϑ, scanning 3-90° 2ϑ, acquisition rate 0.2° 2ϑ/min. The identification of minerals was carried out using the search-match 5.0 JADE software and, for comparison, the JCPDS Data Base (2010).

Physical tests were performed on cubic specimens with side of 15 (± 5) mm were dried at 105 ± 5°C and then the dry solid mass (m_D) were determined.

The real volume was calculated as: $V_R = V_S + V_C$ (where: V_C is the volume of closed pores to helium; V_S is the volume of solid fraction. V_C was determined by helium pycnometer (Ultrapycnometer 1000 model of Quantachrome Instruments). Then, the wet solid mass (m_W) of the samples was determined after water absorption by immersion for 10 days. Through a hydrostatic analytical balance, the bulk volume V_B (with $V_B= V_S+V_O+V_C$) where $V_O= (V_B-V_R)$ is the volume of open pores to helium. V_B is calculated as: $V_B = ((m_W-m_{HY})/\rho wT_{25°C})100$, where m_{HY} is the hydrostatic mass of the wet specimen and $r_W T_X$ is the water density (0,9982 g/cm³) setted at 20°C.

Total porosity (Φ_t), open porosity to water and helium ($\Phi_O H_2O$, $\Phi_O He$ respectively), closed porosity to water and helium ($\Phi_C H_2O$; $\Phi_C He$), bulk density (ρ_B), real density (ρ_R), real specific weight (g_R), solid density (ρ_S), void ratio (e) were computed as:

Φ_T (%) = $[(V_B-V_S)/V_B]100$; $\Phi_O H_2O$ (%) = $[(m_W-m_D)/\rho wT_{25°C}]/V_B)100$; $\Phi_C H_2O$ (%) = Φ_T - $\Phi_O H_2O$; $\Phi_C He$ (%) = Φ_T- $\Phi_O He$; $\rho_S = m_D /V_S$ [g/cm ³]; $\rho_R = m_D /V_R$ [g/cm ³]; $\rho_B = m_D /V_B$ [g/cm ³]; g_R= 9,81[m/s²]; g_R [kN/m³]; $e = (V_C+V_O)/V_S$.

Weight imbibition coefficient (IC_W) and the saturation index (SI) were computed as: $IC_W = ((m_W-m_D)/m_D)100$ [%]; $SI = (\Phi_O He/\Phi_O H_2O)100$ [%].

Punching strength index was determined with Point Load Tester (mod. D550 Controls Instrument) according with the ISRM (1972) and ISRM (1985) on the same pseudo-cubic specimens used for other physical properties (porosity, density, water absorption, etc.). The load was exerted via the application of a concentrated load with two opposing conical punches. Point load strength index (Is) was calculated as: Is = P/De² [N/mm²], where P [N] is the breaking load and De is the "equivalent diameter of the carrot" [mm] with De = 4(WD) / Π [mm], where W and D are the width perpendicular to the direction of the load and the length of the specimen, respectively. The index value is referred to a standard cylindrical specimen with diameter D = 50 [mm] corrected with a shape coefficient (Φ) calculated as: $\Phi = (De/50)^{0.45}$.

The compression resistance (R_C) and the traction resistance (R_T) of the mortar were indirectly calculated (according to ISRM 1972 and ISRM 1985) using the value of normalized punching resistance, with each of them as: $R_C = K\ Is_{(50)}$ [MPa]; $R_T = Is_{(50)} / 0.8$, where K (multiplication coefficient) = 14 (Palmstrom, 1995).

RESULTS

Mineral and petrographic characterization

Stone materials from monument

The macroscopic and mineral-petrographic analyses were carried out on the volcanic and sedimentary rocks, and on the ancient mortars. In Tab. 3 petrographic features of volcanic samples were reported.

Volcanic samples (STS: 14, 18, 20, 22, 24, 25, 28) belong to two different facies: vacuolar and massive (Figs. 5a, 5b). The vacuolar facies (Fig. 6a) shows an oligoporphyric structure with rare phenocrysts (~ 2%) of iddingsitic olivine and plagioclase. The groundmass is holocrystalline with fluidal texture of plagioclase and clinopyroxene microlites. The massive facies (Fig. 6b) shows an oligoporphyric

TABLE 3

Summary scheme of petrographic features defined by polarized microscope analysis on thin sections and geochemical characteristics by ICP-AES chemical analysis (with rock classification) of samples from the Saccargia Basilica and from volcanic outcrops, with rock classifications according to Le Maitre *et alii* (2002) and D.I. range (according to Thorton & Tuttle, 1961).
Minerals abbreviations: Ol = olivine; Opq = opaque minerals; Pl = Plagioclase; Cpx = Clinopyroxene; Mt = magnetite; Ti-Mt = Ti-magnetite. Rock classification abbreviations: TrBa = trachy-basalt; BaTrAn = basaltic trachy-andesite; BaAn = basaltic andesite.

Samples	Facies/ Origin	Petrographic features by microscopic analysis					Geochemical characteristics		
							Rock classification		D.I. range
		Structure	Porphyritic Index (%)	Phenocrysts	Ground mass	Texture	Le Maitre et al. (2002)	Irvine & Baragar (1971)	Thorton & Tuttle (1961)
STS: 14, 20	Massive / Monument	Porphyric	3	Opq (Mt, Ti-Mt), Pl, CPx, Ol	Microcrystalline	Fluidal / pilotaxitic	BaTrAn	Alkaline	53÷56
STS: 15, 18, 22, 24, 25	Vacuolar / Monument	Porphyric	3÷4	Opq (Mt, Ti-Mt), Pl, CPx, Ol	Holocrystalline	Fluidal	BaTrAn	Alkaline	52÷54
PB: 1, 2, 15, 16, 19, 23, 24, 25, 27, 28	Massive / Outcrops	Porphyric	2÷5	Opq (Mt, Ti-Mt), Pl, CPx, Ol	Microcrystalline / holocrystalline	Fluidal / pilotaxitic	BaTrAn, TrBa, BaAn	Subalkaline, alkaline	35÷56
PB: 4, 5, 7, 8, 9, 11, 12, 13, 18, 21, 26	Vacuolar / Outcrops	Porphyric	2÷4	Opq (Mt, Ti-Mt), Pl, CPx, Ol	Microcrystalline / holocrystalline	Fluidal / pilotaxitic	BaTrAn	Subalkaline, alkaline	48÷53

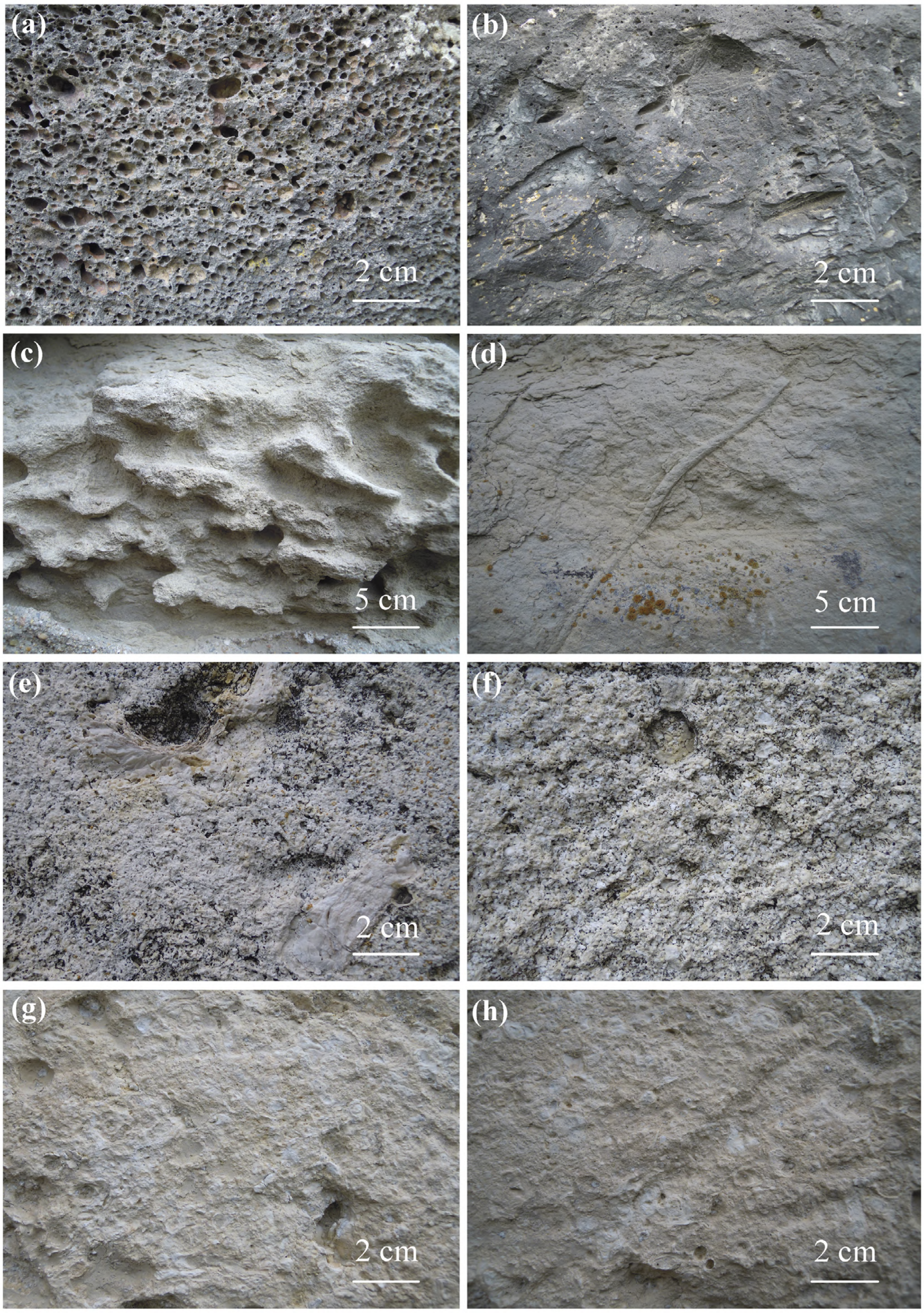

Fig. 5 - Macroscopic features of stone ashlars from the Saccargia Basilica: (a) volcanic vacuolar facies (sample STS 25); (b) volcanic massive facies (sample STS 20); (c) arenaceous marl with differentiated chemical-physical alteration (STS 29); (d) bioturbations (fossil dens) in arenaceous marl (sample STS 17); (e) ostreid bioclasts in limestone (sample STS 37); (f) fossil content (sample STS 37); (g) quartz-feldspar inclusions in limestones (sample STS 19); (h) remains of original plaster on a limestone (sample STS 19).

structure with phenocrysts (< 2%) of very rare olivine with thin iddingsitic rims, and some rare plagioclase. The groundmass is microcrystalline, consisting of fluidal/pilotaxitic texture of plagioclase and clinopyroxene microlites.

About sedimentary rocks, two different lithologies were recognized and following described, in order of abundance. The first lithology (samples STS: 17, 21, 26, 29), more abundant, is an arenaceous marl (Figs. 5c, d) with mud-supported structure (Fig. 6c). Arenaceous / mud fractions consist of sub-angular quartz-feldspar microcrystals (~ 85% of total crystalline phases), also present with size frequently < 80 mm. Bioturbation (also macroscopically visible, Fig. 5d) and bioclasts (~ 10-12% vol.) were also recognized. Bioclasts have a size ranging from 0.1 to 1 mm, with no preferential orientation of disposition, and randomly placed on the section. Bioclasts are attributable to ~ 20% of fragments of bivalves

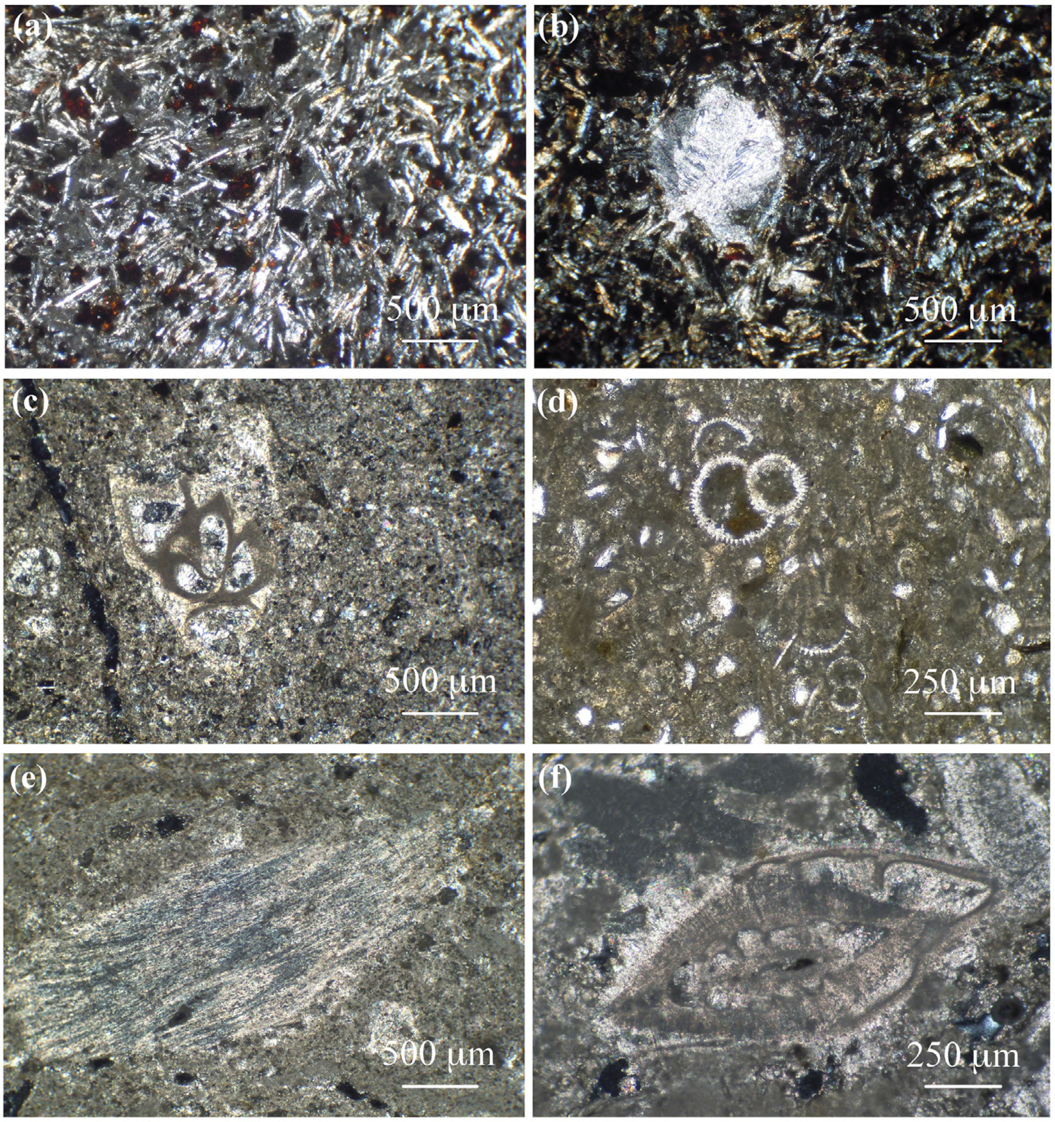

Fig. 6 - Microphotographs of rocks by polarized light microscopy on thin sections (crossed Nicols): (a) groundmass of plagioclase microliths and hiddingsite in basaltic trachy-andesite (sample PB 16); (b) inclusions of Ca-carbonate with calcite micritic spherules in basalt trachy-andesite (sample PB 2); (c) macroforaminifera in marl's mud texture from ashlar of Saccargia Basilica (sample STS 21); (d) bioclastic component in arenaceous marl (sample PC 3); (e) bioclastic fragment in detritic organogenic limestone (sample STS 19); (f) bioclastic fragment in detritic organogenic limestone (sample PC 1).

(Pectinidae), ~ 40% of echinoids and gastropods, ~ 10% of planktonic macroforaminiferas (Fig. 6c) and ~ 15% of corals. Remaining 15% of bioclasts are difficult to identify due to the alteration and very small size (always sub-millimetric). The second lithology (samples STS: 19, 37) consists of organogenic detritic limestone, with variable fossil volume (Figs. 5e, f, g, h). The rock has a recognizable and clear depositional texture with bioclastic components placed in contact forming a frame whose pores are filled by carbonatic cement. The samples often show the presence of quartz-feldspar crystal-clasts with amount varying from 1-2 to 40 vol.% in thin sections. The volume of quartz-feldspar grains is in relation with the outcrop gradual transition between the underlying sands *(Si, Ss)* and these limestones. Locally, the limestone-sand transition is abrupt. The size of crystal-clasts ranges from 2 to 4 mm. They have a well-rounded shape and slight alteration. Bioclast volume ranges from ~ 30% to ~ 60% according to the different limestone facies. Bioclasts (Fig. 6e, f) are attributable to ~ 80% of limestone algae fragments (dimensions of 0.2 mm), ~ 10% of ostreids (from 0.5 mm to 3 cm) and the remaining ~ 10% divided into coral and gastropods fragments (0.5-1 mm) and foraminiferas. The identification of bioclasts is often difficult due to their alteration and small size.

Mortars and plasters from monument

The analysed mortars (samples: STS 32, 33, 36) used to bedding the exterior wall ashlars of Saccargia Basilica show binder/aggregate ratio range ~ 0.35-0.5 calculated trough synoptic method and then confirmed by microscopic analysis on thin section (on average ~ 0.4; Fig. 8a-d).

Macroscopically (Fig. 7a-d), the binder colour generally is whitish CIELAB 65*1*1 in core areas and CIELAB 49*1*2 in external surfaces (Tab. 1). The lime lumps are absent. Cohesion degree is variable from low to medium. The mortars are often fissured with pseudo-parallel micro-fractures in some cases extended throughout the entire surface of the sample. Fractures present a spacing of ~ 0.2 mm and the morphology seems to be linked to a dehydration process rather than mechanical stress. Nevertheless, in some cases the mortar binder has a good compactness. Microscopically, the binder mainly shows a

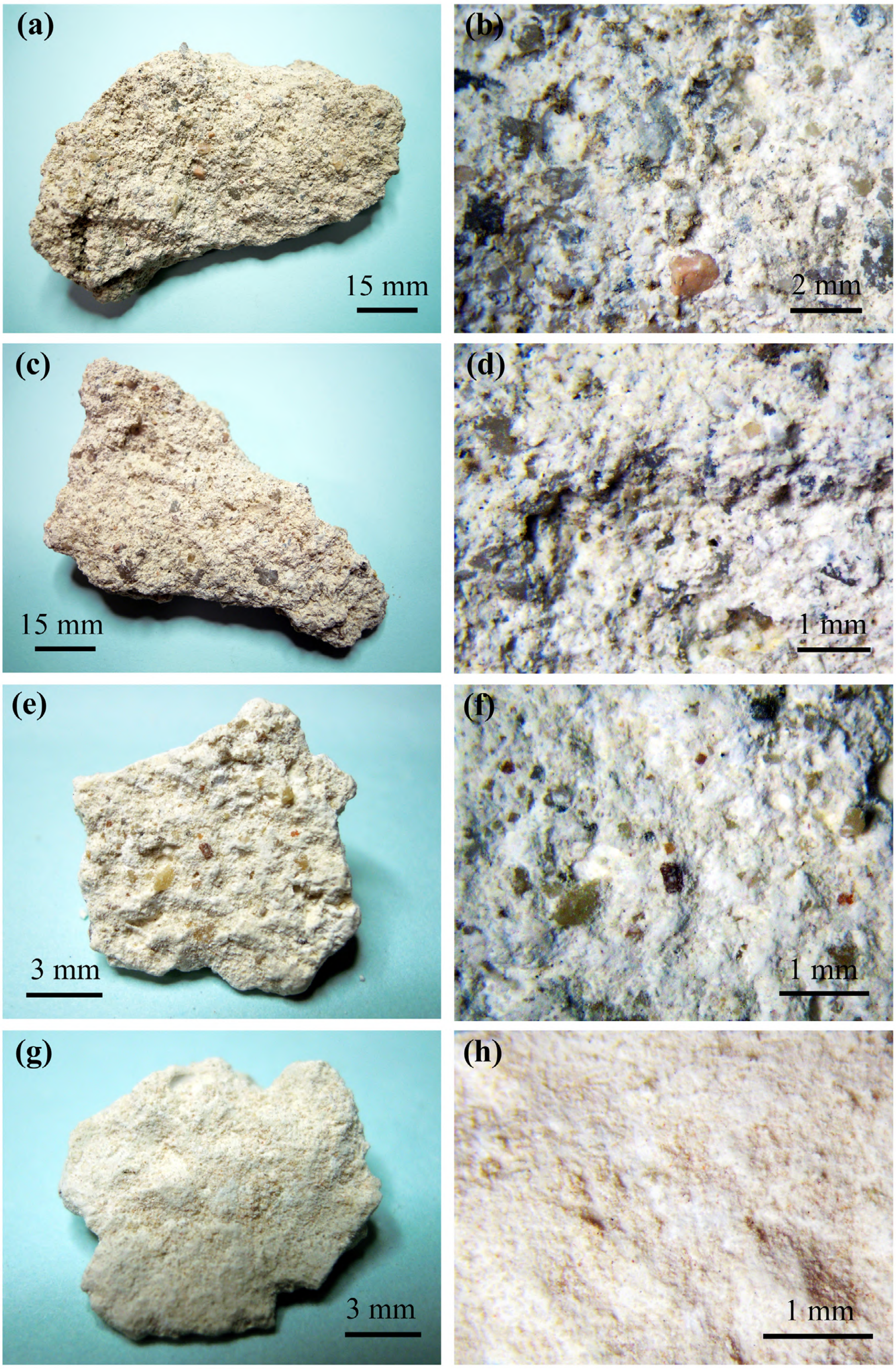

Fig. 7 - Macroscopic features of mortars and plasters from the Saccargia Basilica: (a) mortar (sample STS 32); (b) millimetric size quartz-feldspar aggregates, grey and rose coloured, respectively (sample STS 32); (c) mortar (sample STS 36); (d) millimetric size quartz-feldspar aggregates, grey and rose coloured, respectively (sample STS 36); (e) rinzaffo plaster with B/A ~ 2 (sample STS 1); (f) crystal clasts aggregate in rinzaffo plaster (sample STS 1); (g) arriccio plaster with B/A ratio > 3 (sample STS 3); (h) white binder colouring with submillimetric aggregate in arriccio plaster (sample STS 3). Abbreviations: B = binder; A = aggregate.

calcitic composition, with the presence of some patches where the mineralogical composition can not be detected with the light polarized microscope.

In thin section (Fig. 8a-f), the aggregate of mortars, with a frequently size ranging from 0.1 to 6 mm (Tab. 1), mainly consists of quartz-feldspar crystal-clasts (Fig. 8e) and, clearly subordinate, mafic minerals. Quartz-feldspar aggregate is represented by quartz (~ 70%, frequently size from 0.3 to 3.5 mm, Figs. 8a-d), K-feldspar (~ 28-30%, frequently size from 0.2 to 2 mm, Figs. 8a-d), plagioclase

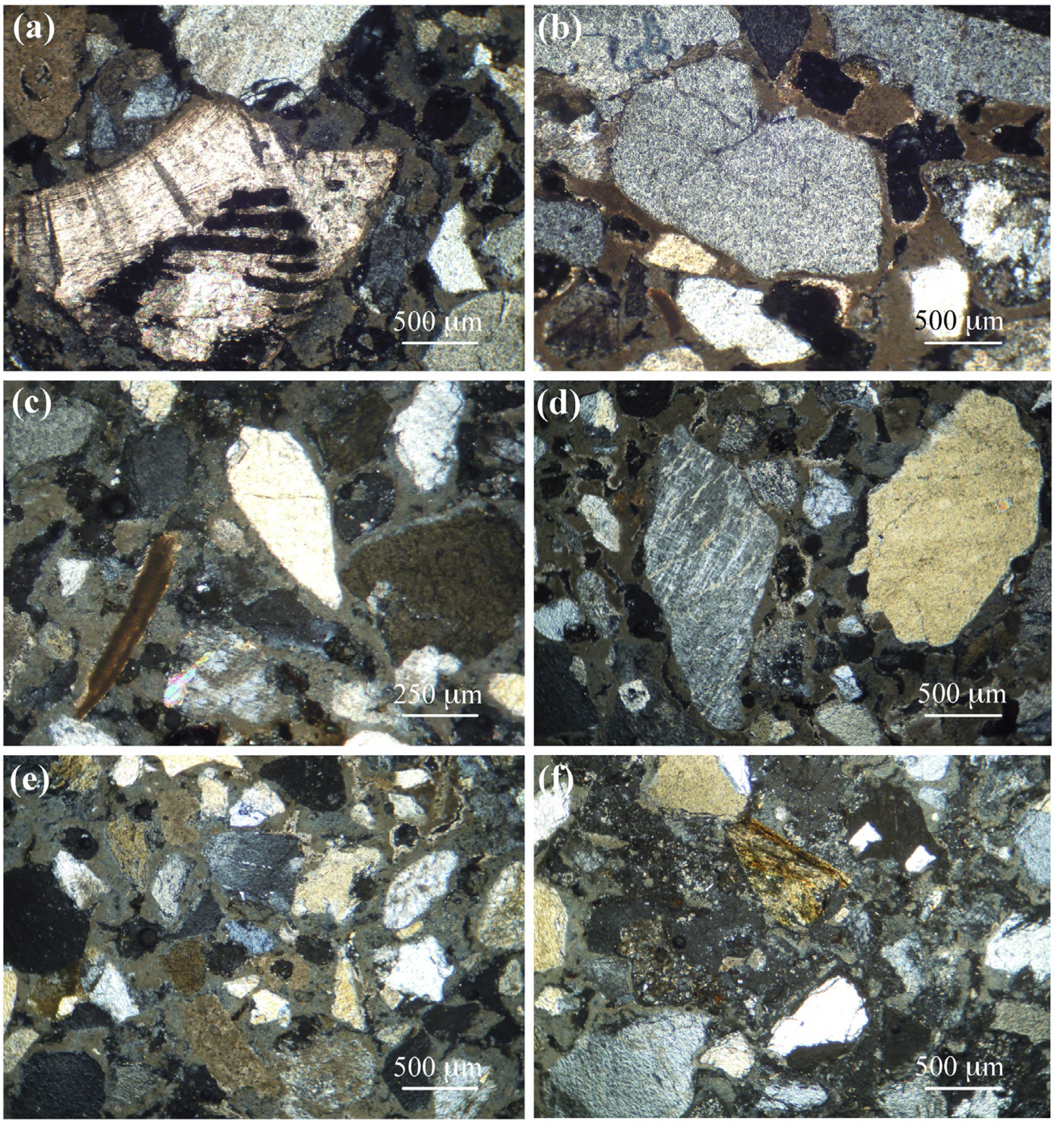

Fig. 8 - Microphotographs of mortars by polarized light microscopy on thin sections (crossed Nicols): (a) bioclasts included in mortar matrix (sample STS 33); (b) quartz-feldspar aggregate (sample STS 32); (c) quartz-feldspar aggregate and bioclastic component (sample STS 33); (d) K-feldspar and quartz crystal-clasts aggregate in mortar (sample STS 36); (e) crystal-clasts aggregate and porosity holes (sample STS 36); (f) alteration processes in the mortar (sample STS 36).

(< 2%, frequently size from 0.1 to 1.5 mm). Quartz-feldspar is poorly altered, with limpid coloration in thin section, sub-roundness shapes (Figs. 8a, b) and low circularity, and sometimes with angular crystals (Figs. 8c, d). Aggregates are moderately selected, according to Folk (1968). Mafic minerals mainly are represented by biotite (< 1%) with size < 0.5 mm. It occasionally is recognized the presence of bioclasts (Fig. 8f), strongly altered, possibly attributable to fragments of echinoids, with dimensions from 0.2 to 3.5 mm.

The *rinzaffo* layers of the plasters (samples: STS 1, 5, 6) used to covering the wall ashlars of monument are more homogeneous and with a higher binder/aggregate ratio (~ 2) with respect to those of the structural mortars, due to their different function in the ancient building. By macroscopic observations (Fig. 7e-f), the *rinzaffo* plaster shows a whitish colour (CIELAB 90*0*-3; Tab. 1) in core of binder. Also in this case the presence of lime lumps is not observed. The cohesion degree is medium. These plasters only rarely are fissured and the micro-fractures are absent. The binder has a lime composition, mainly represented by calcite. The aggregate frequently has a size ranging from 0.1 to 3 mm (Tab. 1), and it mainly consists of silicates (generally as quartz, K-feldspar, plagioclases). Occasional clay minerals (*e.g.*, phyllosilicates of the mica/illite group), in amounts not greater than 3 wt%.

The *arriccio* plaster (sample STS 3) shows a greater binder/aggregate ratio (> 3) with respect to those of the *rinzaffo* plasters, because it used as external layer of the plaster with lower thickness (probable < 6-8 mm). The binder shows a whitish colour (CIELAB 67*0*-3; Tab. 1; Figs. 7h, g), without the presence of lime lumps. Due to the mainly lime composition of binder, the cohesion degree is low. The very fine aggregate shows a low amounts (< 25% by weight of the total sample) with frequently fragment size < 1.5 mm; the silicatic component of aggregate mainly consists of feldspar crystals (*e.g.*, plagioclase) and subordinate quartz.

Stone materials from outcrops

Vacuolar volcanic samples (*e.g.*, PB: 1, 2, 4, 5, 26), from the Meilogu sub-region, show a porphyritic structure due to the presence of phenocrysts of iddingsitic olivine and plagioclase. Groundmass essentially consists of crystalline microlites of plagioclase and clinopyroxene with rare interstitial glass. Samples sometimes include rare secondary carbonate and patches in groundmass (Fig. 6b). Massive volcanic samples, or weakly vacuolar, (*e.g.*, PB 15, 16, 19, 28), show a weakly porphyric structure for presence of olivine phenocrysts (with very thin iddingsitic rim), and rarer plagioclase, sometimes zoned, immersed in a fluidal groundmass consisting of plagioclase microlites. Opaque minerals are relatively abundant.

Marl samples collected from the outcrops of Logudoro sub-region, (north Sardinia) are typical arenaceous marls consisting of a micritic mud matrix. Marls belong to the *arenaceous marls units (Uma)*, outcropping around Florinas area, before described by Mazzei & Oggiano (1990). According to these authors, this formation consists of a more or less dense alternation of marly layers (from centimetres to meters) from grey to grey-whitish colours, with silty layers (on average decimetre order), fairly well-cemented. The colour varies from yellowish to light beige to greenish.

Limestones samples were collected from outcrops located at south and north-west of *Florinas* (northern Sardinia), at the top of minor reliefs as Mt. Sorighe, Mt. Chieia. The detritic-organogenic limestones consist of two units; *Upper (Cs)* and *Lower (Ci)*. The geological units only differ about the stratigraphic location, and both lay on sandy units *(Si, Ss)* with predominantly sub-horizontal or slightly inclined layers.

The composition of limestones is very heterogeneous. In outcrop, stratigraphy often is recorder a lateral heterotopic facies passage with strong variations of bioclasts volume and cohesion characteristics. As in monument rocks, outcrop limestones facies represent transition lithologies between sand layers *(Si, Ss)*, introducing a variable volume of quartz-feldspar clasts.

Bioclasts consist of ostreids, pettinids, echinoderms, gastropods and corals.

Geochemical features and classification of volcanic rocks

Tables 4a and 4b report the major and trace element data and the CIPW normative mineralogy of monument and outcrop samples. Table 3 shows (beyond the petrographic features) a synthesis of the geochemical characteristics including the rock classifications according to the Total Alkali Silica diagram of Le Maitre *et alii* (2002).

In the variation diagrams of Fig. 9, wt% major elements *vs*. the differentiation index (D.I. of Thornton & Tuttle, 1960) of volcanic rocks from monument and outcrops were reported. The monument's samples (STS: 14, 15, 18, 20, 22, 24, 25) show similar geochemical characteristics with part of samples from the outcrops (PB: 1-9, 11-13, 15, 16, 18, 19, 21, 23, 26), constituting a main population (within the elliptical dotted line) with D.I. between 47 and 57. However, internally to this population, some samples (PB 2, 8, 9, 12, 21) get out of it, showing for different wt% values of following element oxides: Fe_2O_3, CaO, MgO, Na_2O, K_2O (Fig. 9; Tab. 4a). Other samples from outcrops (PB: 24, 25, 27, 28) are less differentiated than the samples shown above, showing D.I. values between 34 and 43.

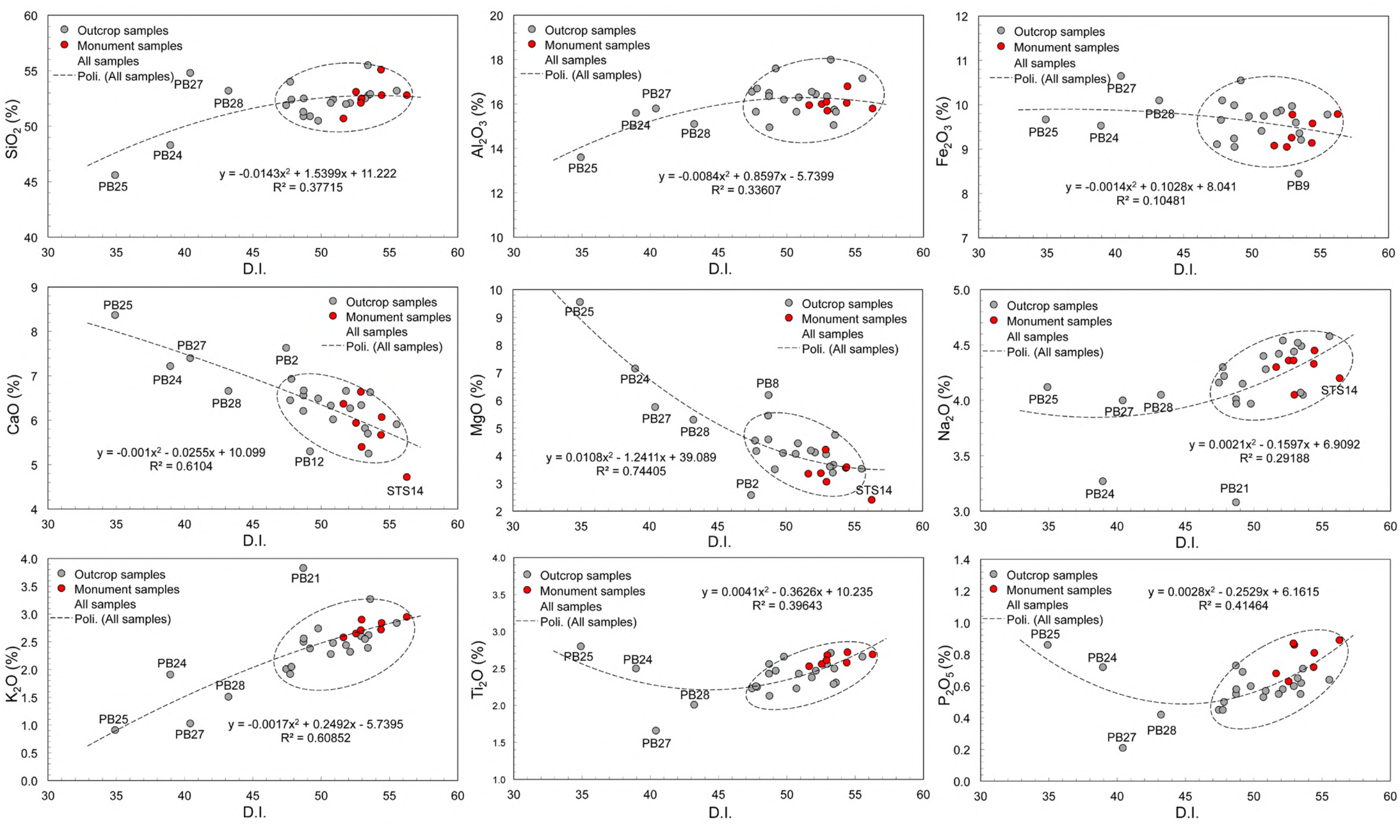

Fig. 9 - Variation diagrams: major elements (wt%) vs. differentiation index of Thornton & Tuttle, 1960 (where D.I. = normative Q +Ab + Or + Ne + Kp + Lc) for the volcanic samples from the monument and outcrops.

TABLE 4A

Chemical analysis data of volcanic rocks sampled from the Saccargia Basilica and from volcanic outcrops (see Fig. 4), where reported: the rock classification according to TAS diagram of LE MAITRE *et alii* (2002), wt% of major elements, C.I.P.W. normative mineralogy and the following parameters: S.I. (wt% Solidification Index of KUNO, 1966) = (MgO•100)/ (MgO+FeO$_{tot}$+Na$_2$O+K$_2$O); A.I. (Agpaitic Index of SHAND, 1951) = (Na$_2$O+K$_2$O)/Al$_2$O$_3$; D.I. (Differentiation Index of THORNTON & TUTTLE, 1960) = normative Q +Ab + Or + Ne + Kp + Lc; SAL = sum of sialic minerals; FEM = sum of mafic minerals. Rock classification abbreviations as caption of Table 3.

Sample	STS25	STS22	STS15	STS20	STS24	STS18	STS14	PB18	PB23	PB24	PB4	PB7	PB8	PB21	PB3	PB16	PB1	PB12	PB15	PB5	PB11	PB13	PB26	PB19	PB25	PB28	PB9	PB2	PB27
Classification	BTrAn	BTrAn	BTrAn	BTrAn	BTrAn	BTrAn	BTrAn	BTrAn	BTrAn	TrBa	BTrAn	BTrAn	BTrAn	BTrAn	BTrAn	BTrAn	BTrAn	BTrAn	BTrAn	BTrAn	BTrAn	BTrAn	BTrAn	BTrAn	TrBa	BTrAn	BTrAn	BTrAn	BaAn
SiO_2	52.1	50.7	52.8	53.1	52.5	55.1	52.8	50.9	52.9	48.3	52.4	50.5	52.5	51.3	52.4	53.2	52.8	50.9	52	52.1	52.1	52.4	52.5	54	45.6	53.2	55.5	51.9	54.8
TiO_2	2.61	2.53	2.72	2.56	2.68	2.58	2.69	2.56	2.31	2.5	2.56	2.66	2.13	2.43	2.43	2.66	2.5	2.47	2.38	2.47	2.23	2.25	2.71	2.26	2.8	2.01	2.29	2.23	1.66
Al_2O_3	16.1	15.95	16.8	16	15.7	16.05	15.8	16.5	15.65	15.6	16.35	16.2	14.95	16.35	16.3	17.15	15.75	17.6	16.55	16.45	15.65	16.7	18	15.65	13.6	15.1	15.05	16.55	15.80
Fe_2O_3	9.26	9.08	9.58	9.05	9.78	9.14	9.79	9.99	9.21	9.53	9.97	9.74	9.05	9.24	9.75	9.78	9.36	10.55	9.83	9.87	9.41	10.1	9.6	9.66	9.67	10.1	8.45	9.11	10.65
MnO	0.12	0.1	0.11	0.1	0.1	0.1	0.08	0.11	0.11	0.12	0.12	0.11	0.12	0.12	0.11	0.1	0.08	0.16	0.11	0.11	0.12	0.12	0.13	0.1	0.14	0.11	0.13	0.08	0.12
MgO	6.64	6.37	6.07	5.94	5.4	5.67	4.72	6.56	6.63	7.22	6.34	6.49	6.67	6.21	6.02	5.91	5.25	5.3	6.66	6.27	6.33	6.93	5.82	6.45	8.37	6.66	5.70	7.63	7.4
CaO	4.22	3.35	3.59	3.37	3.06	3.56	2.41	4.59	4.75	7.15	4.05	4.1	6.19	5.45	4.45	3.53	3.67	3.51	4.19	4.12	4.07	4.17	3.61	4.55	9.55	5.3	3.39	2.58	5.76
Na_2O	4.36	4.3	4.45	4.36	4.05	4.33	4.2	4.01	4.05	3.27	4.44	3.97	3.97	3.08	4.28	4.58	4.49	4.15	4.42	4.54	4.4	4.22	4.52	4.3	4.12	4.05	4.07	4.16	4.00
K_2O	2.71	2.58	2.84	2.65	2.9	2.72	2.95	2.5	3.27	1.91	2.6	2.74	2.56	3.83	2.48	2.84	2.62	2.38	2.44	2.32	2.28	2.05	2.55	1.92	0.91	1.51	2.39	2.01	1.03
P_2O_5	0.87	0.68	0.81	0.63	0.86	0.72	0.89	0.55	0.71	0.72	0.6	0.6	0.58	0.73	0.57	0.64	0.62	0.69	0.55	0.58	0.53	0.5	0.65	0.45	0.86	0.42	0.55	0.45	0.21
L.O.I.	1.99	2.31	1.18	1.5	2.49	0.92	2.18	0.3	0.53	3.01	0.92	1.16	0.65	2.42	0.17	0.87	1.65	2.33	0.83	0.06	0.65	0.87	1.36	0.75	3.23	0	1.41	2.43	0.02
Total	100.98	97.95	100.95	99.26	99.52	100.89	98.51	98.57	100.12	99.33	100.35	98.27	99.37	101.16	98.96	101.26	98.79	100.04	99.96	98.89	97.77	100.31	101.45	100.09	98.85	98.46	98.93	99.13	101.45
S.I.	29.97	29.59	27.47	28.02	25.39	26.93	22.7	29.58	29.67	34.24	28.22	29.39	31.09	28.82	27.78	26.57	25.13	24.71	29.62	28.33	29.32	30.93	26.89	30.03	37.68	31.08	28.7	34.52	33.42
D.I.	52.9	51.63	54.43	52.55	52.96	54.38	56.27	48.7	53.59	38.95	52.93	49.78	48.72	48.69	50.87	55.53	53.47	49.18	51.82	52.12	50.7	47.82	53.31	47.73	34.91	43.21	53.42	47.44	40.41
MgVal.	0.59	0.58	0.56	0.57	0.52	0.55	0.49	0.57	0.59	0.6	0.56	0.57	0.59	0.57	0.55	0.54	0.53	0.5	0.57	0.56	0.57	0.58	0.55	0.57	0.63	0.57	0.57	0.62	0.58
CIPW Norm with ratio $Fe_2O_3/FeO = 0.15$																													
Q	0	0	0	0	1.55	1.67	3.3	0	0	0	0	0	0	0	0	0	0	0	0	0	0	0	0	0	0	0.02	4.86	0.36	0.48
C	0.41	1.62	1.82	1.34	2.39	1.23	3.45	0.17	0	0	0.31	0.69	0	0	0	1.66	0.34	3.47	0.34	0.37	0	1.15	2.8	0	0	0	0.92	3.92	0
Or	16.01	15.25	16.78	15.66	17.14	16.07	17.43	14.77	19.32	11.29	15.36	16.19	15.13	22.63	14.65	16.78	15.48	14.06	14.42	13.71	13.47	12.11	15.07	11.35	5.38	8.92	14.12	11.88	6.09
Ab	36.89	36.38	37.65	36.89	34.27	36.64	35.54	33.93	34.27	27.67	37.57	33.59	33.59	26.06	36.21	38.75	37.99	35.11	37.4	38.41	37.23	35.71	38.24	36.38	23.24	34.27	34.44	35.2	33.84
An	15.25	12.18	12.52	12.6	9.56	12.96	6.14	19.18	14.87	22.25	16.17	16.42	15.41	19.48	17.94	13.33	14.16	12.9	17.19	16.65	16.22	17.42	13.66	17.73	15.93	18.56	13.22	9.86	22.11
Ne	0	0	0	0	0	0	0	0	0	0	0	0	0	0	0	0	0	0	0	0	0	0	0	0	6.29	0	0	0	0
Di	0	0	0	0	0	0	0	0	2.24	4.8	0	0	6.34	1.52	0.22	0	0	0	0	0	0.27	0	0	1.02	15.23	2.61	0	0	2.65
Ed	0	0	0	0	0	0	0	0	1.05	2.1	0	0	2.99	0.75	0.12	0	0	0	0	0	0.14	0	0	0.53	5.58	1.45	0	0	1.50
Sl	0	0	0	0	0	0	0	0	3.29	6.9	0	0	9.34	2.27	0.34	0	0	0	0	0	0.41	0	0	1.55	20.82	4.07	0	0	4.15
En	6.98	9.34	9.61	13.74	13.45	14.12	11.75	6.17	5.05	5.24	6.29	6.89	5.24	6.52	7.92	7.89	10.3	11.92	5.51	6.36	8.71	11.51	9.63	14.68	0	15.38	14.2	19	17.20
Fs	3.58	4.91	5.54	7.66	9.04	8.33	9	3.6	2.72	2.63	3.8	3.85	2.83	3.69	4.98	4.86	6.87	9.52	3.2	3.88	5.14	6.82	5.84	8.74	0	9.82	7.93	8.83	11.14
Hy	10.56	14.25	15.14	21.39	22.49	22.45	20.75	9.78	7.77	7.87	10.09	10.74	8.07	10.22	12.89	12.75	17.17	21.43	8.71	10.23	13.85	18.33	15.47	23.43	0	25.2	22.13	27.84	28.34
Fo	6.7	4.57	3.86	0.74	0	0	0	7.12	7.3	7.37	6.66	6.5	5.91	5.77	4.89	4.79	1.95	0.9	7.76	6.49	4.86	4.03	3.41	0.64	9.66	0	0	0	0
Fa	3.79	2.65	2.45	0.45	0	0	0	4.58	4.34	4.08	4.43	4	3.53	3.6	3.39	3.25	1.43	0.79	4.96	4.36	3.16	2.63	2.28	0.42	4.48	0	0	0	0
Ol	10.48	7.21	6.32	1.19	0	0	0	11.71	11.64	11.45	11.08	10.5	9.44	9.37	8.28	8.04	3.38	1.69	12.72	10.85	8.02	6.66	5.69	1.06	14.13	0	0	0	0
Mt	1.6	1.57	1.65	1.56	1.69	1.58	1.69	1.72	1.59	1.64	1.72	1.68	1.56	1.59	1.68	1.69	1.61	1.82	1.69	1.7	1.62	1.74	1.66	1.67	1.67	1.74	1.46	1.57	1.84
Il	4.96	4.81	5.17	4.86	5.09	4.9	5.11	4.86	4.39	4.75	4.86	5.05	4.05	4.62	4.62	5.05	4.75	4.69	4.52	4.69	4.24	4.27	5.15	4.29	5.32	3.82	4.35	4.24	3.15
Ap	2.02	1.58	1.88	1.46	1.99	1.67	2.06	1.27	1.65	1.67	1.39	1.39	1.34	1.69	1.32	1.48	1.44	1.6	1.27	1.34	1.23	1.16	1.51	1.04	1.99	0.97	1.27	1.04	0.49
SAL	68.56	65.43	68.77	66.49	64.91	68.57	65.86	68.05	68.46	61.2	69.41	66.89	64.13	68.17	68.81	70.52	67.97	65.55	69.35	69.14	66.92	66.39	69.77	65.46	50.84	61.77	67.57	61.21	62.52
FEM	29.61	29.41	30.16	30.47	31.25	30.6	29.61	29.34	30.32	34.28	29.14	29.36	33.79	29.76	29.12	29.01	28.35	31.23	28.92	28.82	29.37	32.16	29.47	33.03	43.93	35.8	29.21	34.68	37.97

TABLE 4B

Chemical analysis data of volcanic rocks sampled from the Saccargia Basilica and from volcanic outcrops, where reported the ppm of trace elements and the rock classification according to TAS diagram of LE MAITRE *et alii* (2002). Rock classification abbreviations as caption of Table 3.

Sample	STS25	STS22	STS15	STS20	STS24	STS18	STS14	PB18	PB23	PB24	PB4	PB7	PB8	PB21	PB3	PB16	PB1	PB12	PB15	PB5	PB11	PB13	PB26	PB19	PB25	PB28	PB9	PB2	PB27
Classification	BTrAn	BTrAn	BTrAn	BTrAn	BTrAn	BTrAn	BTrAn	BTrAn	BTrAn	TrBa	BTrAn	BTrAn	BTrAn	BTrAn	BTrAn	BTrAn	BTrAn	BTrAn	BTrAn	BTrAn	BTrAn	BTrAn	BTrAn	BTrAn	TrBa	BTrAn	BTrAn	BTrAn	BaAn
Ba	1060	1080	1155	1070	1290	1165	1260	1015	1260	1610	1125	1195	970	1605	986	1180	1115	1385	994	949	935	849	1015	770	1425	592	1020	749	329
Ce	75.6	77.4	82.3	78	91.2	82.4	91	70.9	98.4	111	84.1	86.4	84.8	111	74.7	85.5	79.8	118	75.6	68	76.7	68.1	77.7	57.6	132.5	51.1	74.1	57.5	28.3
Cr	80	90	60	60	70	90	80	60	100	300	60	70	230	220	50	30	80	120	70	70	120	90	20	80	380	160	60	70	160
Cs	0.2	0.27	0.29	0.29	0.31	0.2	0.45	0.55	0.33	0.19	0.12	0.19	0.21	0.22	0.03	0.29	0.09	0.05	0.11	0.06	0.07	0.12	0.09	0.1	0.72	0.15	0.17	<0.01	0.46
Dy	3.96	4.15	4.36	4.09	4.89	3.94	6.03	4.15	4.2	4.31	4.38	4.74	4.52	4.45	4.08	4.24	3.82	7.12	4.34	4.2	4.43	4.15	5.13	4.13	5.04	3.87	4.26	3.47	3.48
Er	1.57	1.83	1.62	1.45	1.92	1.42	2.69	1.7	1.67	1.79	1.78	1.98	1.85	1.82	1.72	1.83	1.4	2.8	1.81	1.77	2.02	1.59	2.2	1.68	2.17	1.82	1.72	1.34	1.55
Eu	2.56	2.72	2.85	2.45	3.07	2.64	3.45	2.6	2.57	2.61	2.44	2.72	2.49	2.59	2.37	2.88	2.38	3.99	2.58	2.63	2.7	2.37	3.07	2.23	2.6	2.24	2.6	1.95	1.61
Ga	22.3	22.8	24.5	23.2	26.3	24.1	27	22	22.3	21.1	23.6	24.1	21.4	22.5	22.9	24.4	22.4	24.7	23.7	23.7	22	23	24.1	21.9	18.5	22.5	22.9	21.3	21.2
Gd	6.56	6.54	7.14	6.76	8.07	6.6	9.87	5.79	6.37	6.17	6.58	7.45	6.67	6.92	6.12	7.41	6.01	10.8	6.76	6.27	6.93	5.75	8.29	5.65	6.77	5.84	7.09	5.44	4.45
Hf	5.4	5.5	6.1	5.5	6	5.4	6.3	5.3	6.4	7.2	5.5	6	5.9	7.1	5	6.4	5	6.1	5.8	5.1	5.7	4.9	6	4.5	8.1	4.4	5.3	4.1	3.3
Ho	0.58	0.67	0.64	0.63	0.69	0.61	1.01	0.71	0.64	0.76	0.76	0.78	0.82	0.78	0.68	0.78	0.58	1.15	0.76	0.72	0.83	0.59	0.93	0.6	0.82	0.7	0.67	0.63	0.63
La	39	41.7	44.1	40	46.3	43.9	58.9	36.1	49.1	58.5	47.1	45.6	42.6	63.2	43.1	43.1	39.9	69.4	38.2	35.4	41.4	34.4	54.5	29.1	68.1	25.7	41.3	27.4	14.5
Lu	0.11	0.14	0.15	0.1	0.14	0.11	0.22	0.18	0.15	0.2	0.18	0.21	0.2	0.18	0.17	0.2	0.12	0.27	0.19	0.17	0.22	0.17	0.23	0.15	0.25	0.17	0.15	0.17	0.18
Nb	51	52.6	57.2	52.2	62.2	57	62.4	46.9	46.3	55.9	52.4	54.4	47.4	53.2	47.2	52.9	52.8	46.5	41.4	41.4	41.8	39	45.1	36.1	69.6	31.5	46.3	37.2	15.1
Nd	39	41	43.4	40.6	48.9	43	56	36.9	45.1	48.2	42.7	46.1	42.8	50.7	38.4	45	40.2	75.4	43.8	36.8	40.6	37.1	49.2	31.6	54.2	29.1	41.2	29.5	17.1
Pr	8.89	9.08	9.61	9.01	10.9	9.94	12.2	8.27	11.15	12.6	9.88	10.75	9.95	12.8	8.85	10.35	9.25	17.2	9.53	8.42	9.14	8.31	11.25	7.08	14.15	6.31	9.25	6.56	3.61
Rb	51.4	54.9	58.9	54.8	63.5	56.9	67.1	53.2	68.2	10.9	51.8	55.4	57.1	72.8	41.9	63.4	51.8	52.2	53.3	44.9	41.9	46.1	46.4	41.2	60.8	33	52.2	31.5	29.2
Sm	7.76	8.16	8.16	8.02	9.78	8.11	10.1	7.9	8.56	8.13	8.11	8.8	9.02	8.38	7.52	9.32	7.66	14.85	8.96	7.99	8.67	7.55	9.76	7.08	8.68	6.38	8.38	6.19	4.74
Sn	1	2	2	2	2	2	2	2	2	2	2	2	2	2	2	2	2	2	2	2	1	2	2	2	2	1	1	1	1
Sr	1110	1205	1205	1170	1185	1230	1310	1255	1050	1140	1175	1335	1065	1025	1090	1375	1160	956	1095	1145	935	1045	1135	988	1165	731	1080	906	476
Ta	3.4	3.5	3.4	3.4	3.5	3.3	3.7	2.7	2.6	3.3	3.4	3	3	3.1	3	3	3.1	2.5	2.4	2.3	2.6	1.9	2.9	1.9	4.2	1.8	3.1	1.9	0.8
Tb	0.77	0.87	0.8	0.78	0.96	0.78	1.11	0.83	0.81	0.86	0.86	0.95	0.85	0.89	0.88	0.93	0.76	1.43	0.89	0.83	0.86	0.79	0.96	0.79	0.94	0.8	0.84	0.69	0.65
Th	5.21	5.16	5.62	5.15	6.31	5.22	6.19	5.07	5.51	7.16	5.92	5.69	5.43	6.79	5.11	5.51	5.62	5.44	4.89	4.45	4.65	3.91	5.08	3.91	8.09	3.27	4.93	4.2	2.62
Tm	0.12	0.14	0.15	0.13	0.14	0.12	0.25	0.21	0.22	0.25	0.23	0.25	0.23	0.25	0.19	0.24	0.17	0.38	0.24	0.23	0.26	0.18	0.28	0.22	0.32	0.23	0.13	0.18	0.22
U	0.62	0.93	0.8	0.98	1	0.54	0.88	0.71	1.32	1.67	1.24	0.6	0.75	0.72	0.43	0.73	0.57	0.85	0.55	0.49	1.09	0.94	0.84	0.62	1.92	0.83	1.07	0.56	0.65
V	114	126	124	119	142	122	136	144	134	162	136	146	135	149	125	135	119	151	143	136	135	180	133	137	195	143	124	129	140
W	7	1	1	1	1	1	1	1	1	1	1	1	1	1	1	1	1	15	1	1	1	1	1	1	12	1	1	1	1
Y	16.1	18.1	17.9	16.9	19	17.8	31.9	18.3	17.8	19.1	23.2	21.8	21	21	18.9	20.2	15.9	31.4	19.2	19	22.5	18.3	25.5	17.3	21.9	17.7	19.6	16	16
Yb	1.02	1.21	1.15	0.95	1.17	0.96	1.49	1.29	1.07	1.24	1.39	1.24	1.4	1.36	1.12	1.2	0.9	1.84	1.28	1.14	1.48	1.13	1.49	1.05	1.55	1.15	1.25	1.09	1.08
Zr	221	235	262	235	271	249	278	231	268	316	244	265	264	317	216	275	238	257	248	219	258	230	254	180	354	176	239	175	137

All the analysed samples show typical chemical characters of the Plio-Pleistocenic transitional and sub-alkaline series of north Sardinia volcanism (Beccaluva *et alii*, 1975, 1976, 2013). Among the monument samples, the transitional "basalts" (STS: 20, 22, 25) show the following compositional range: SiO_2 ranging from 50.7 to 53.1 wt%; TiO_2 from 2.53 to 2.61 wt%, the sum of the alkalis from 6.88 to 7.07 wt% (Tab. 4a). These latter always have normative olivine and hypersthene ranging from 1.2-10.5% to 10.6-21.4%, respectively (Tab. 4a). The subalkaline rocks (STS: 14, 18, 24) present following value ranges: SiO_2 from 52.5 to 55.1 wt%, TiO_2 from 2.58 to 2.69 wt%, sum of the alkali from 6.95 to 7.15 wt%. The sub-alkaline character is confirmed by the presence of normative quartz and hypersthene ranging from 1.5 - 3.3% to 20.7- 22.5%, respectively (Tab. 4a). The normative corundum amount of monument samples ranges from 0.4 to 3.5%, suggesting a change of original chemical composition for the alteration processes of volcanic rock, or for pollutions with artificial material used to construct the Basilica (*e.g.*, mortars).

According to the TAS classification scheme (Le Maitre *et alii*, 2002), all the monument specimens fall into the field of basaltic trachy-andesite (Tab. 4a; Fig. 10).

The samples from the volcanic outcrops show a serial character from sub-alkaline to transitional, to weakly alkaline, to alkaline, typical of the Sardinian Plio-Pleistocenic volcanism. Subordinately, there are lavas with sub-alkaline character, in agreement with the literature (Beccaluva *et alii*, 1981). The transitional "basalts" (PB: 1, 3-5, 7, 8, 11-13, 15, 16, 18, 19, 21, 23, 24, 26) show SiO_2 range from 55.5 to 48.3 wt% (Tab. 4a), TiO_2 from 2.13 to 2.71 wt%, and total alkalis from 5.18 to 7.42 wt%. The tholeiitic character of these samples is confirmed by the presence of normative olivine and hypersthene ranging from 1.1 to 12.7% (ol) and from 7.8 to 23.4% (hy) (Tab. 4a). According to TAS scheme, these samples outcrop samples are mainly represented by basaltic trachy-andesite, except two trachy-basalts (PB: 24, 25; Tab. 4a; Fig. 10).

The sub-alkaline "basalts" (PB: 2, 9, 27, 28) are characterized by SiO_2 ranging from 51.9 to 55.5 wt%, TiO_2 from 1.66 to 2.29 wt% (Tab. 4a), total alkalis from 5.03 to 6.46 wt%. The presence of normative quartz and hypersthene indicates their sub-alkaline character with values from 0.02 to 4.9 (qz) and from 22.1 to 28.3 (hy), Tab. 4a. According to the TAS (Fig. 10), the samples were classified as basaltic trachy-andesite (PB: 2, 9, 28), basaltic andesite (PB 27).

The alkaline "basalt" (PB25) shows following chemical values: SiO_2 = 45.6 wt%; TiO_2 = 2.80 wt%; sum of alkalis = 5.03 wt%. It has normative nepheline (6.3%) and olivine (14.1%), Tab. 4a. According to the classifications of Le Maitre *et alii* (2002) PB25 sample is classified as trachy-basalt (Fig. 10).

XRPD analysis and alteration of materials

Analytical results of selected representative building materials, from data acquired by X-Ray diffractometry technique, are reported and discussed on the following, for providing information about the primary mineralogy of the rock and secondary mineral phases occurred on the stone surface of Basilica due to alteration processes. Table 5 reports on the analytical data obtained for different type of materials and associated alteration, according to the following scheme: 1) unaltered ("fresh") carbonatic rocks, 2) altered carbonatic rocks, 3) unaltered original mortars, 4) altered original mortars. Due to the absence of decay and of any alteration mineralogical transformations, data of the volcanic rocks do not reported in the Table 5.

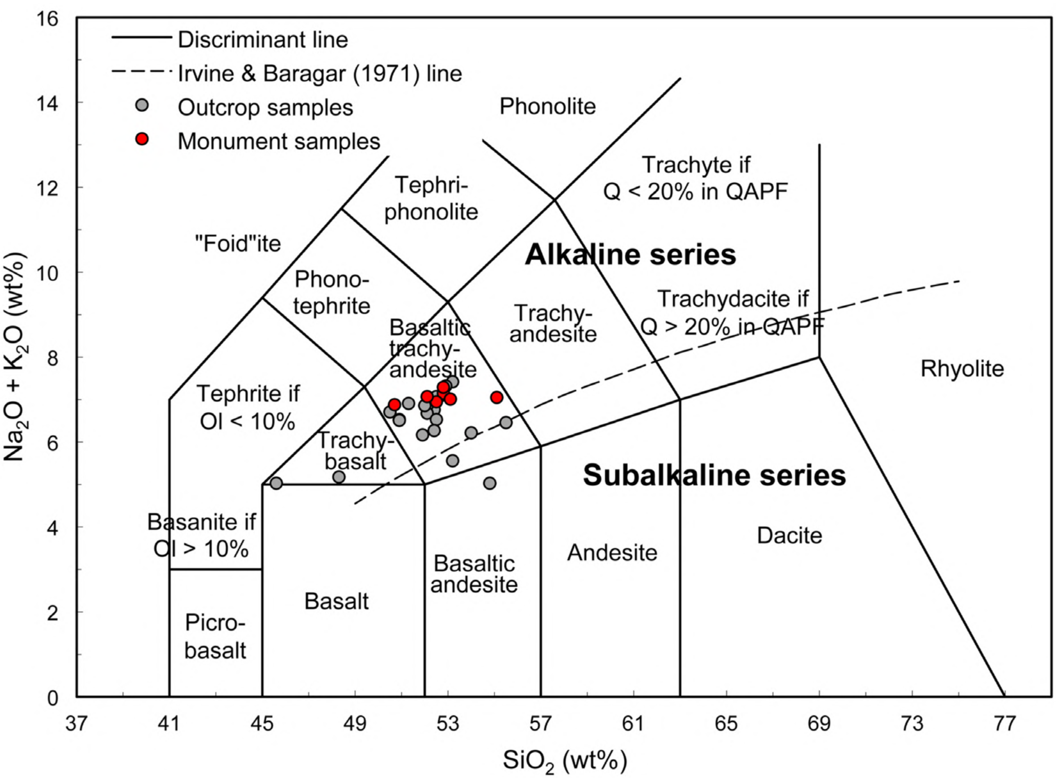

Fig. 10 - Volcanic rock classification diagram, where plotted the samples from the monument and outcrops: Total Alkali-Silica diagram [(Na_2O+K_2O) vs. SiO_2 wt%] of Le Maitre *et alii* (2002).

The analysed materials revealed a quite simple mineral composition both for unaltered/altered carbonatic rocks that mainly reflects the original mineralogical assemblage of these lithologies, also due to the low concentration of secondary crystalline phases on the surface of stone with respect to the minerals of the stone substrate.

Analyses performed on the unaltered lithotypes show the presence of a quantitatively variable fraction of carbonate minerals (such as calcite, dolomite, etc.) and silicate minerals (such as feldspars, quartz, micas, etc.) belonging to the arenaceous fraction. The main mineral assemblage (Tab. 5) can locally change, even from ashlar to ashlar, according to the changing of the place of supply. The common mineral association of unaltered limestones (STS 13, 19; Fig. 11) mainly consists of calcite, locally in association with traces of mica/illite group minerals. The mineral assemblage of unaltered marls (STS 17; Fig. 12) consists of lower calcite than the limestones, dolomite, and subordinate feldspar (with also plagioclase) and quartz.

Observing the altered samples of the marls, the main newly formed minerals due to alteration belong to the clay group minerals and sulphates. The former group include mica/illite and/or smectite (montmorillonite-nontronite series) group phases (sample STS 17 and 29; Tab. 5; Fig. 12). They are quite uncommon and generally occur in percentages less than 10%. Sulphates occur as gypsum, generally in black crusts, also in percentages less than 10%.

The mortars and the plasters are often affected by chemical alteration processes. In the case of mortar sample STS 3, 5 (Tab. 5; Fig. 13) the mineral composition of original unaltered samples widely varies from zone to zone of the monument, and generally consists of silicates, carbonates, in different associations and amounts. Silicates generally occur as quartz, plagioclases and K-feldspar, which commonly form the aggregate of original mortars, and occur in very different proportions.

The amount of silicate minerals ranges from < 15 wt% (*i.e.*, plasters) to about 75 wt% (*i.e.*, mortars), according to the binder/aggregate ratio planned by the constructor. Clay group minerals generally are uncommon and occur as phyllosilicates of the mica/illite group, in amounts not greater than 2-3% by weight of the total sample.

Regarding to carbonate phases, calcite is the only mineral occurring in the original mortars of Saccargia Basilica and it represents the composition of the binder. It is quantitatively dominant in most of analysed mortars, frequently exceeding 60 wt%, up to be the only crystalline phase of the binder in some lime based samples (*i.e.*, plasters).

The main chemical-mineralogical alteration processes on the mortars and plasters, especially in the lime binder, are the dissolution and the sulfation. The secondary phases are represented by clay group minerals, occur as mica/illite and/or smectite (montmorillonite-nontronite series) group phases, in percentage less than 10 wt% (samples STS 1, 6; Tab. 5; Fig. 13). Sulphates (only as gypsum) also occur as main secondary mineral. In such cases, gypsum percentage in the sample is greater than 30 wt% (sample STS 6; Fig. 13), with the formation of typical surface Ca-sulphate crusts (sometimes with greyish or blackish colours) and consequent exfoliation and loss of material.

TABLE 5

Mineral assemblage from X-Ray Diffraction (*XRPD*) data of representative selected building materials collected from: unaltered/altered limestones, marls and original mortars and plasters of Saccargia Basilica.
Abbreviation legend: Pl = plagioclase; Qz = quartz; Kf = potassium feldspar; Mi/Il = Micas (including biotite, muscovite, illite); Ca = calcite; Gy = gypsum; Do = dolomite.

Sample	Material	Description	Type	Major (≥ 40 wt%)	Minor (40 > wt% ≥ 10)	Trace (< 10 wt%)
STS 13	Unaltered rocks	Rock substrate	Limestone	Ca	-	-
STS 16				Ca	Qz, Do, Pl	Kf
STS 19				Ca	-	Mi/Ill
STS 26			Marl	Ca	Kf, Pl	Mi/Ill, Do
STS 17	Altered rocks	Outer crust (or patina)	Marl	Ca, Qz	-	Do, Pl, Mi/Ill
STS 29				Ca, Qz	Pl	Mi/Ill, Sm, Gy
STS 32	Unaltered samples	Mortar substrate	Mortar	Qz	Pl, Kf, Ca	-
STS 33				Qz	Pl	Mi/Ill
STS 3		Plaster substrate	Plaster	Ca	-	Pl
STS 5				Ca	Qz	Pl, Kf
STS 30	Altered samples	Outer crust (or patina)	Mortar	Ca	Pl	Gy, Sm, Mi/Ill
STS 1			Plaster	Ca	Qz	Gy, Pl
STS 6				Ca, Gy	-	Qz, Mi/Ill

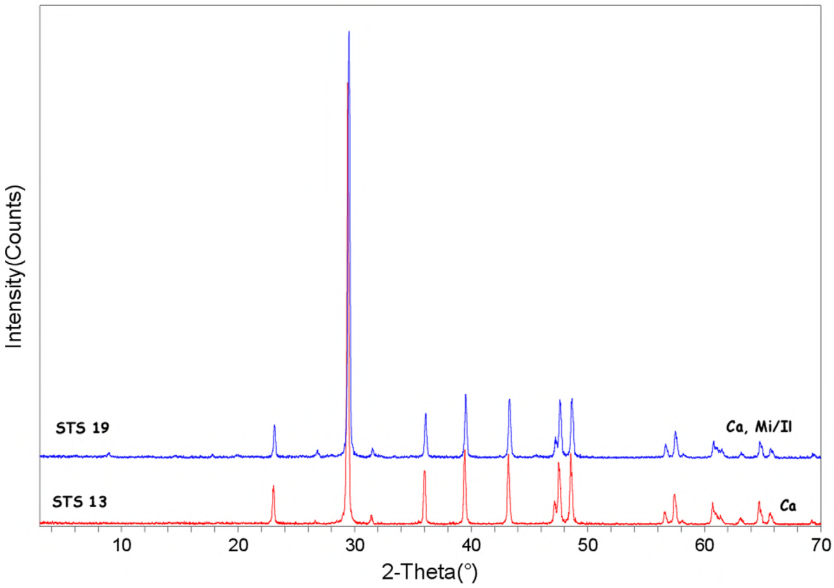

Fig. 11 - XRPD pattern with typical mineral composition of some unaltered limestones (samples STS 13, 19) from the Saccargia Basilica (Codrongianos). Abbreviation legend: Mi/Il = Micas (including biotite, muscovite, illite); Ca = calcite.

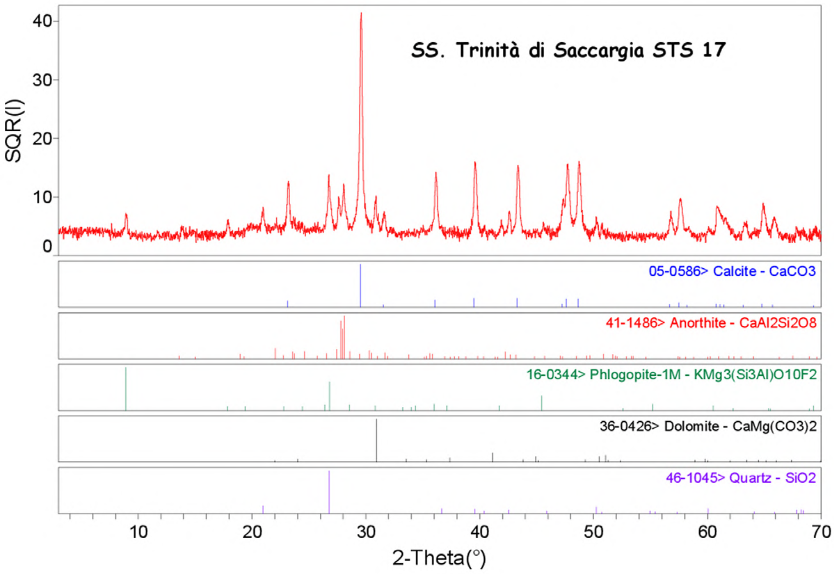

Fig. 12 - XRPD pattern of the marl sample STS 17 taken on ashlar alteration crust from the Saccargia Basilica (Codrongianos).

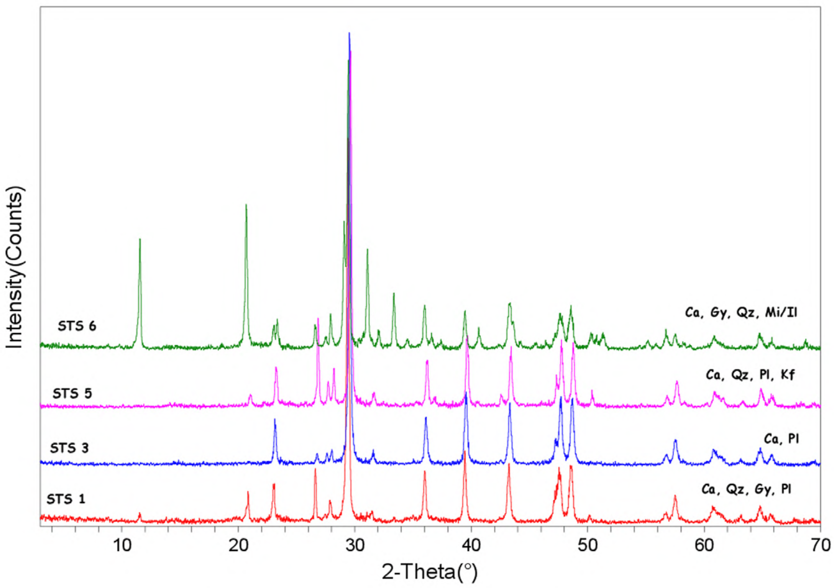

Fig. 13 - XRPD pattern with typical mineral composition of unaltered plasters (samples STS: 3, 5) and altered plasters (samples STS 1, 6) from the Saccargia Basilica (Codrongianos). Abbreviation legend: Pl = plagioclase; Qz = quartz; Kf = potassium feldspar; Mi/Il = Micas (including biotite, muscovite, illite); Ca = calcite; Gy = gypsum; Do = dolomite.

Physical properties

Results of physical analysis of monument and outcrop samples have been reported in Table 6.

Volcanic samples from monument, mainly represented by vacuolar facies, show a greater average total porosity of 23.3 ± 2.8% (Fig. 14a) with respect to outcrops volcanic rocks with average 11.3 ± 5.0% (Tab. 6). In all volcanic samples, the total porosity framework is represented by about 20% of helium closed porosity and about 80% of helium open porosity.

Solid density and also the real density of volcanic samples show high values (Tab. 6; Fig. 14b), due to the presence of mafic minerals with high density (clinopyroxene: on average 3.4 g/cm^3; opaques (magnetite): 5.1 g/cm^3). The monument samples have following value ranges: 2.94-3.01 and 2.83-2.87 g/cm^3, respectively, with means of 2.97 ± 0.03 g/cm^3 and 2.85 ± 0.01 g/cm^3 (Tab. 6). The outcrop samples show a more variability of values with higher standard deviations: 2.84-3.10 g/cm^3 and 2.80-3.04 g/cm^3, respectively, with means of 2.97 ± 0.10 and 2.88 ± 0.08 g/cm^3 (Tab. 6). Real density is also affected by closed porosity ranging from 2.6 to 5.3% in case of monument (Tab. 6; Fig. 14b, c), and from 0.4 to 7.6% in the case of outcrops. The higher variability of density values in these latter is due to their higher compositional heterogeneity.

The averages of saturation index are higher in volcanic outcrop samples (61.3 ± 15.8%; Tab. 6; Fig. 14d) respect to monument samples (42.7 ± 7.2%), due probably to a higher heterogeneity of the composition and vesicularity in former samples. The total absorption test shows that saturation of the lithotype is 95% completed after about 72 hours immersion. For all samples, anyway saturation index is less than 100% (Fig. 14d), indicating the absence or minor amount of high-hygroscopic minerals in rocks matrix as salts.

The imbibition coefficients generally are similar in a range from 1.7 to 5%. This parameter shows a lesser standard deviation in monument volcanics (0.3 *vs.* 0.7%).

The graphics where plotted Point Load Strengh Index (PLT) *vs.* total porosity and PLT Index *vs.* bulk density for all analysed samples (Fig. 14e, f) shows negatively/positively correlation with coefficients between two parameters respectively of R^2 exp = 0.43, 0.55 (Fig. 14e, f). Due to a greater total porosity (Fig. 14a) related to the different vesicularity, the volcanic rocks from monument have a lower PLT Index with respect to outcrop samples: 3.69 ± 1.34 MPa *vs.* 7.88 ± 1.18 MPa (Tab. 6).

Within each group of sedimentary rocks, density values and porosity mainly affect by the different textural

TABLE 6

Physical and mechanical properties of samples taken from the Saccargia Basilica, outcrops and mortars. *Classification according to TAS diagram (Le Maitre *et alii*, 2002).
Symbol legend: ρ_S = solid density; ρ_R = real density; γ_R = real specific weight; ρ_B = bulk density; $\Phi_O H_2O$ = open porosity to water and helium; $\Phi_O He$ = open porosity to helium; $\Phi_C He$ = closed porosity to water; $\Phi_C He$ = closed porosity to helium; Φ_T = total porosity; e = void ratio index. S.D. = standard deviation.

Sample		Lithology	ρ_S (g/cm^3)	ρ_R (g/cm^3)	γ_R (kN/m^3)	ρ_B (g/cm^3)	$\Phi_O H_2O$ (%)	$\Phi_O He$ (%)	$\Phi_C He$ (%)	Φ_T (%)	e -	CI_w (%)	SI (%)	Is_{50} (MPa)	R_C (MPa)	R_T (MPa)
STS 24	MONUMENT	Basaltic trachy-andesite*	2.98	2.83	27.79	2.27	10.8	19.9	5.3	25.2	0.31	4.8	54.5	2.53	35.41	3.16
STS 20			3.01	2.87	28.12	2.12	9.4	26.0	5.2	31.2	0.42	4.5	36.3	5.91	82.7	7.38
STS 22			2.94	2.87	28.12	2.14	10.4	25.4	2.6	28.0	0.38	4.9	41.1	3.48	48.65	4.34
STS 18			2.96	2.84	27.91	2.25	9.1	20.8	4.2	25.1	0.32	4.0	43.7	3.76	52.7	4.71
STS 14			2.95	2.86	28.05	2.16	9.3	24.4	3.0	27.5	0.36	4.3	38.2	2.79	39	3.48
		Mean	2.97	2.85	28	2.19	9.8	23.3	4.1	23.3	0.36	4.5	42.8	3.69	51.69	4.62
		S.D.	0.03	0.01	0.14	0.07	0.8	2.8	1.2	2.8	0.04	0.3	7.2	1.34	18.7	1.67
PB 25	OUTCROPS	Trachy-basalt*	3.01	2.88	28.29	2.64	6.4	8.5	4.3	12.7	0.14	2.4	74.8	5.82	81.46	7.27
PB 1		Basaltic trachy-andesite*	3.06	2.94	28.82	2.46	8.2	16.4	4.3	20.7	0.25	3.4	50.1	7.81	109.28	9.76
PB 15			2.85	2.8	27.49	2.62	4.4	6.4	1.8	8.2	0.09	1.7	67.9	8.5	119.05	10.63
PB 16			3.05	2.84	27.84	2.62	5.3	7.7	7.6	15.3	0.17	2.0	68.4	8.26	115.65	10.33
PB 26			2.96	2.87	28.14	2.28	8.1	20.6	3.1	23.6	0.30	3.6	39.6	6.49	90.79	8.11
PB 28			2.84	2.83	27.79	2.6	5.3	8.3	0.4	8.7	0.09	2.0	62.9	9.33	130.68	11.67
PB 2			2.88	2.82	27.62	2.55	7.8	9.3	2.1	11.4	0.13	3.1	84.1	8.01	112.1	10.01
PB 19			3.1	3.04	29.79	2.64	5.6	13.1	2.2	15.3	0.18	2.1	42.4	8.82	123.51	11.03
		Mean	2.97	2.88	28.22	2.55	6.4	11.3	3.2	11.3	0.17	2.5	61.3	7.88	110.32	9.85
		S.D.	0.1	0.08	0.76	0.13	1.5	5.0	2.2	5.0	0.07	0.7	15.8	1.18	16.53	1.48
STS 19	MONUMENT	Limestone	2.82	2.76	27.05	1.88	21.7	31.9	5.2	37.1	0.54	11.5	67.9	0.56	7.91	0.71
STS 37			2.75	2.73	26.81	1.94	26.3	29.0	1.3	30.3	0.42	13.5	90.6	1.99	27.86	2.49
STS 17		Arenaceous marl	2.75	2.7	26.45	2.16	16.7	20.0	2.0	22.0	0.27	7.8	83.5	2.47	34.52	3.08
STS 29			2.76	2.65	25.99	2.27	12.8	14.5	4.4	18.9	0.22	5.7	88.4	3.14	44.01	3.93
STS 26			2.75	2.71	26.63	2.29	14.2	15.8	1.3	17.1	0.20	6.2	89.9	3.36	46.98	4.19
STS 21			2.76	2.63	25.8	2.36	8.3	10.4	4.8	15.2	0.17	3.5	74.3	4.21	58.94	5.26
PC 1	OUTCROPS	Limestone (*Ci*)	2.86	2.74	26.88	2.43	9.1	11.4	4.3	15.7	0.18	3.8	79.9	0.36	4.99	0.45
PC 2			2.84	2.72	26.67	2.44	8.9	10.3	4.3	14.6	0.16	3.6	86.3	2.09	29.32	2.62
PC 5		Limestone (*Cs*)	2.86	2.73	26.76	2.05	19.2	25.0	4.8	29.8	0.40	9.4	76.7	0.91	12.76	1.14
PC 6			2.87	2.73	26.75	2.31	12.8	15.4	5.2	20.6	0.24	5.5	82.8	1.35	18.87	1.69
PC 7			2.87	2.75	26.98	1.9	28.8	31.2	4.1	35.3	0.51	15.2	92.4	0.85	11.9	1.06
PC 8			2.87	2.67	26.19	2.41	9.2	9.9	7.4	17.3	0.19	3.8	93.4	1.29	18.06	1.61
PC 3		Arenaceous marl (*Uma*)	2.84	2.63	25.84	2.07	18.5	21.4	7.7	29.2	0.37	9.0	86.4	1.8	25.17	2.25
PC 4			2.84	2.64	25.88	2.06	19.4	22.0	7.5	29.5	0.38	9.4	88.1	0.85	11.95	1.07
PC 9			2.77	2.68	26.34	2.43	8.3	9.4	3.2	12.5	0.14	3.4	88.2	4.3	60.18	5.37
STS 33	MONUMENT	Mortar	2.81	2.74	26.85	1.98	23.2	27.6	4.3	31.9	0.42	11.7	84.3	1.21	16.91	1.51
STS 36			2.77	2.63	25.84	1.89	23.7	28.2	4.4	32.6	0.47	12.6	84.3	0.33	4.68	0.42
STS 32			2.73	2.62	25.67	2.14	16.5	18.4	1.9	20.2	0.28	7.7	89.9	2.06	28.89	2.58
		Mean	2.77	2.66	26.12	2	21.2	24.7	3.5	24.7	0.39	10.7	86.1	1.2	16.82	1.5
		S.D.	0.04	0.07	0.64	0.12	4.1	5.5	1.5	5.5	0.10	2.6	3.2	0.86	12.11	1.08

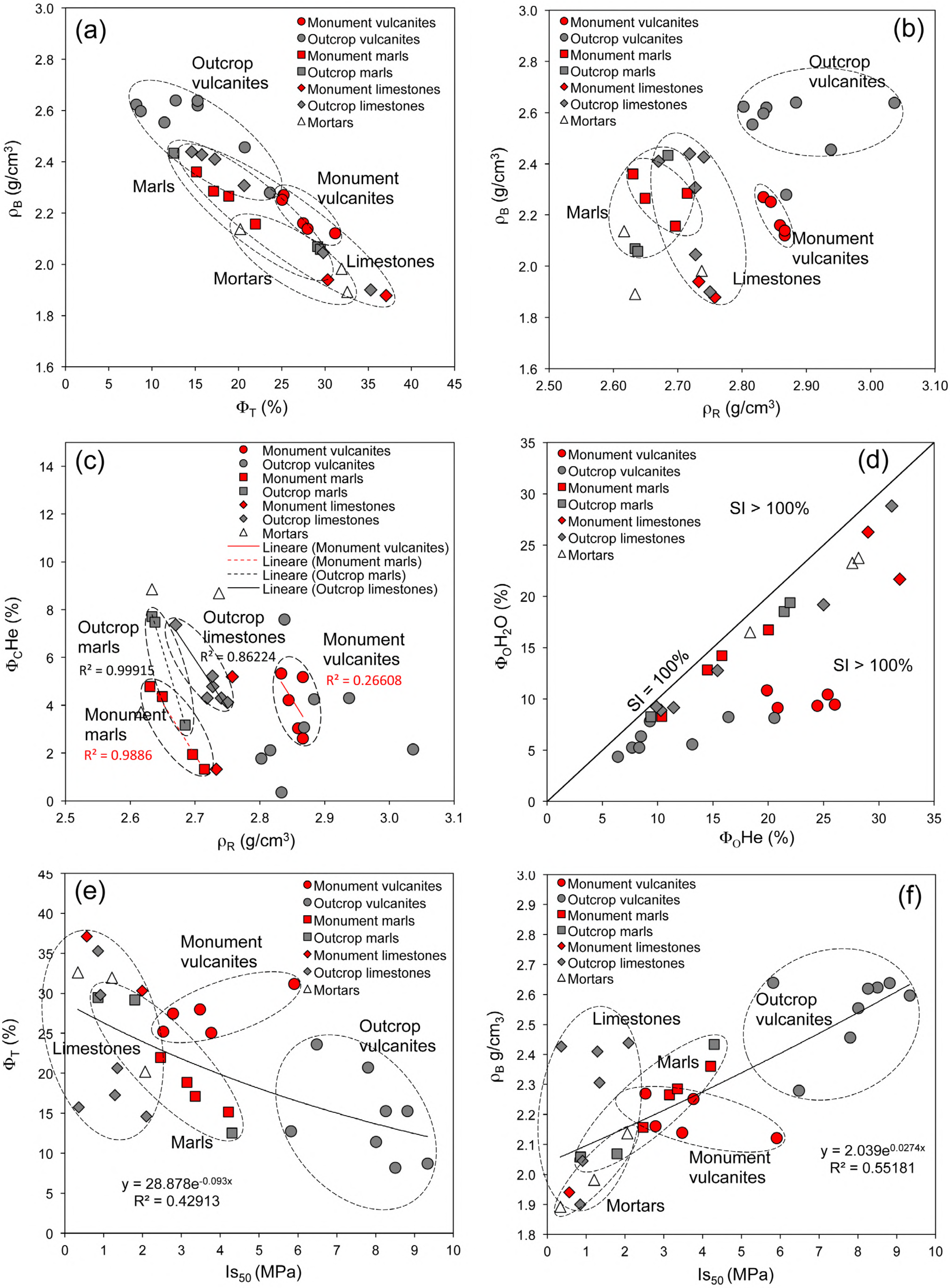

Fig. 14 - Physical and mechanical features of samples from the monument and the outcrops: (a) total porosity vs. bulk density; (b) real density vs. bulk density; (c) real density vs. helium closed porosity; (d) open helium porosity vs. open water porosity (with saturation index represented); (e) point load strength index (Is50) vs. total porosity; (f) point load strength index (Is50) vs. bulk density.

and microstructural aspects: mud-supported in case of arenaceous marls and carbonatic cementation in case of detritic-organogenic limestones.

Limestones from monument show greater total porosity (33.7 ± 4.8%; Figs. 14a) with respect to outcrop rocks (17.2 ± 8.9%), without a proportional ratio between the helium closed and open porosities. The marl samples of monument show a total porosity mean of 18.3 ± 0.04%, while the outcrop samples have a mean of 23.7 ± 9.7% (Tab. 6).

Solid density of monument and outcrop limestones shows values of 2.79 ± 0.05 g/cm^3 and 2.86 ± 0.01 g/cm^3, respectively. The marls have 2.76 ± 0.01 g/cm^3 and 2.81 ± 0.04 g/cm^3, respectively (Tab. 6). These high values of solid density are justified, in addition to the calcite (with density of 2.71 g/cm^3), by the presence of arenaceous, clay and mud fractions (10-35%) represented by quartz, feldspar and especially phyllosilicates (with density of 2.6-2.9 g/cm^3) and other phases (Fe-oxides and hydroxide) with higher density (2.9-5.3 g/cm^3).

The monument and outcrop limestone samples show values of real density between 2.67 and 2.76 g/cm^3 (Tab. 6; Fig. 14b, c), while the marls show lower values, between 2.63 and 2.71 g/cm^3.

The means of saturation index are similar in limestones of monument and outcrop samples (79.2 and 85.3%; Fig. 14d), as well as in the marl samples (84.0 and 87.6%).

Due to their greater porosity, the monument limestone samples show an imbibition coefficient (about 12.5%) higher than outcrops (6.9%), Tab. 6. Instead, following the inverse behaviour, the monument marl samples show an imbibition coefficient (5.8%) lower than outcrops (7.3%).

The monument and outcrop samples of limestone show similar values of mechanical strength with PLT Index of 1.28 ± 1.01 and 1.14 ± 0.59 MPa, respectively (Tab. 6; Fig. 14e, f). The monument samples of marls show higher values of mechanical strength (PLT index = 3.29 ± 0.72 MPa) with respect to the outcrop samples (2.32 ± 1.78 MPa), due to higher total porosity in these latter.

DISCUSSION

According to the chemical TAS classification (Fig. 10), supported by mineralogical and petrographic analysis, the analysed volcanic rocks of the Saccargia Basilica are basaltic trachy-andesites. The volcanic outcrops have more compositional variability represented by trachy-basalt, basaltic andesite and basaltic trachy-andesite.

The variation diagrams of Fig. 9, reporting the plot of major elements *vs.* differentiation index (D.I.), show that the most of samples have a homogeneous chemical composition (see the main population within the elliptic dashed line in the graphic of Fig. 7), while some samples (PB: 24, 25, 27, 28) show a different geochemical behaviour in all graphics with respect to the monument and other outcrop samples. Also other samples (PB: 2, 8, 9, 12, 21) show minor different geochemical characteristics with respect to the main sample population, for diverse wt% values of some major elements: CaO, MgO, Fe_2O_3, Na_2O, K_2O respectively (Fig. 9). Except for the most differentiated sample (STS14 - a trachyte with D.I. 56.27; Tab. 4a; Fig. 9), that shows lower amounts of CaO and MgO, the analysed monument samples are very similar to some sampled outcrops.

In Fig. 15 the binary diagrams of trace elements and some major elements have been reported. The basaltic trachy-andesites (*i.e.,* STS: 15, 20, 22, 24, 25, 18) from the monument and the outcrop samples (PB: 1, 3, 4, 5, 7, 11, 13, 15, 16, 18) form a homogeneous population with similar composition (Fig. 15), while the samples PB: 2, 8, 9, 12, 19, 21, 23-28 have different geochemical behaviour with respect to the monument samples. For this reason, the outcrops of these latter samples can be excluded as probable origin of basaltic trachy-andesites from the monument. The basaltic trachy-andesite (STS 14), falling outside the main sample population above described, shows a geochemical similarity with outcrop sample PB 12 (Fig. 15), then it is possible that these samples have the same origin.

Even he monument samples do not show particular chemical alteration processes, to disregard any possible change of geochemical data, we have also considered some further diagrams which considers the ratios of some immoble trace elements (Nb/Y *vs.* SiO_2, Zr/TiO_2 *vs.* SiO_2; Figs. 16a, b) and the following ratios: Nb/Y *vs.* Zr/TiO_2, Nb/Zr *vs.* Th/Ta shown in Fig. 15. These graphics confirmed the considerations made above with exception of sample PB 18 that shows a different ratio Nb/Y, and for this it has been excluded as probable supply point of raw materials.

On the base of petrographic features observed by microscopic analysis, the basaltic trachy-andesites from monument show a greater petrographic similarity (*i.e.,* texture and structural aspects) with the samples PB: 1, 5, 21, belonging to the following localities, respectively: *Su Paris de Coloru* (Codrongianos), 500 m north from the Basilica; *Planu e Filighe* (southeast of Ploaghe village), 7.2 km southeast from the Basilica (Tab. 2; Fig. 4). Considered the longer distance from the monument, the chemical results and some petrographic differences (*e.g.,* lower size of plagioclases and pyroxenes of groundmass, minor vesicularity), the outcrop of the sample PB 21 (from Borutta field, about 16.7 km from the Basilica) has been definitively excluded as possible supply area.

The basaltic trachy-andesitic sample STS 18 from the monument (Tabs. 3, 4a) shows a petrographic similarity of the outcrop basaltic trachy-andesitic samples PB: 2, 9, 13, 19. But, as highlighted before, the samples PB 2 and PB 9 can be excluded, due to their different chemical composition (Fig. 15), it is probable that the monument sample STS 18 comes from the outcrop of samples PB 13 or PB 19 belonging to the following localities: *Scala Torta* (Siligo), 8.5 km south-east from the Basilica (Tab. 2; Fig 4); *Charchidanas* (Codrongianos), 3.1 km from the Basilica.

The basaltic trachy-andesitic sample STS 14 from the monument shows a petrographic similarity with the basaltic trachy-andesitic outcrop samples (PB: 1, 12, 20, 21), but considering its greater geochemical similarity with sample PB 12 (Figs. 7, 15), the STS 14 sample probably comes from the outcrop of *Scala Torta* locality (Siligo), located at 8.3 km from the Basilica (Tab. 2; Fig. 4).

Accordingly, as the compositional variety of the volcanics from monument belong to different supply areas, the choice of materials can be possibly done in different outcrops during the construction of the Basilica, or for its ancient maintenance, modifications and renovations followed one another over time. A single place or quarry of extraction of the materials has

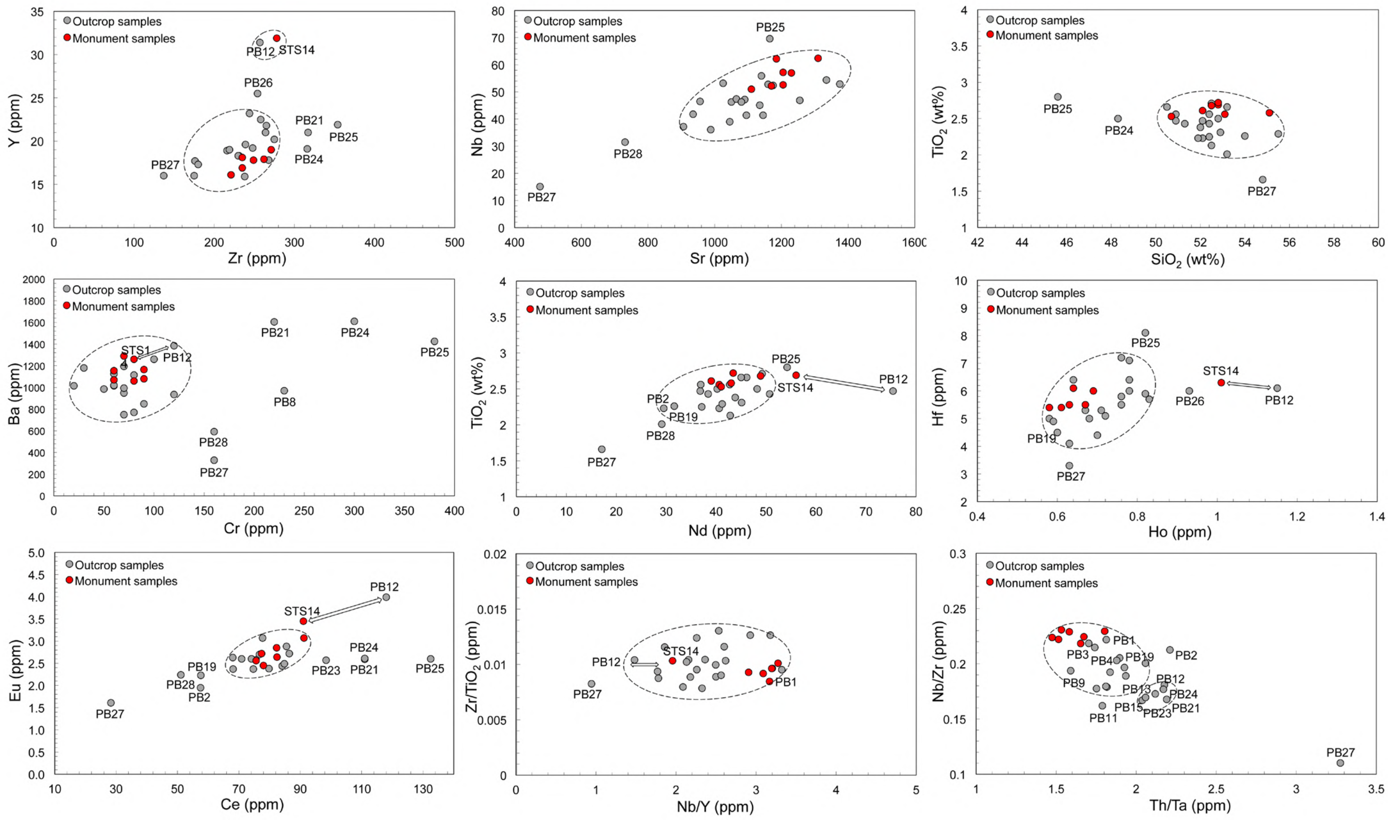

Fig. 15 - Binary diagrams of trace elements and some major elements used to chemical discrimination of the volcanic samples from the monument and outcrops: Y vs. Zr, Nb vs. Sr, TiO2 vs. SiO_2, Ba vs. Cr, TiO_2 vs. Nd, Hf vs. Ho, Eu vs. Ce, Zr/TiO_2 vs. Nb/Y, Nb/Zr vs. Th/Ta.

therefore to be rejected. However, it is reasonable to assume that the volcanic stones of the Basilica mainly come from close outcrops, and subordinately from erratic stone boulders taken from the field, also in view of lower transport costs of materials.

Moreover, the monument volcanic samples show a greater vesicularity than the samples on field, indicating that the constructors possibly preferred the porous volcanic facies, because they are easy workable to realise ashlar. However, the monument samples have a lower point load strength index (3.69 ± 1.34 MPa; Tab. 6) than the field samples (7.88 ± 1.18 MPa), due to their great total porosity (Fig. 14a).

The sedimentary lithologies used in the construction of the monument are similar to marls and limestones samples collected from outcrops of Logudoro sub-region (north Sardinia), where, between the different facies of marls, limestones, essentially present the same two distinct lithologies used in the monument construction. The mineral-petrographic integration of data, obtained from optical microscopy and XRPD analyses, considering both monument samples and geomaterials cropping out in Florinas-Codrongianos area, shows strong similarities in rock texture and mineralogical association (*e.g.*, with similar compostional ratios of quartz, plagioclase, dolomite and mica/illite group minerals). Moreover, bioclastic component also shows strong similarity (Figs. 5, 6) in both lithologies. The amount and variety of some bioclastics (ostreids, pettinids, echinoderms, gastropods and corals and the algae in the limestones, bioturbation (fossil dens) in the marls), certainly have greatly supported the recognition of the stone facies. In the monument and field samples, the same transition facies between sand and limestone layers occurs, as well as the amount of quartz-feldspar intraclasts.

In both sedimentary rocks, the physical-chemical alteration is mostly localized on the surface of the ashlars and occurs in several decay forms (*e.g.*, alveolization, exfoliation, decohesion). The decay forms, along with the weathering factors (rainfall and/or capillary rising, washout), favour the chemical action onset on matrix cement of rock, which starts and enhances the dissolution or transformation of the original minerals and the re-precipitation in newly formed phases (*i.e.*, sulphates, as gypsum, mica/illite and/or smectite group phases), generally concentrated as surface patinas. However, due to their different textural and microstructural features, the limestones and arenaceous marls used as ashlars in the Basilica show a different physical behaviour and alteration degree. The marls from monument, having a lower total porosity (< 20%) than the limestones (~ 34%), show a greater mechanical strength than the physical decay. Moreover, due to different composition, mainly consisting of silicate carbonate mud, the dissolution processes are lesser frequent than in the limestones.

Thus, the association of the basaltic stone and sedimentary rocks reproduces in the Saccargia Basilica a differential erosion, in which the syngenetic and secondary porosity is an important factor of chemical-physical decay, because it favours the passage of salt solutions (capillary

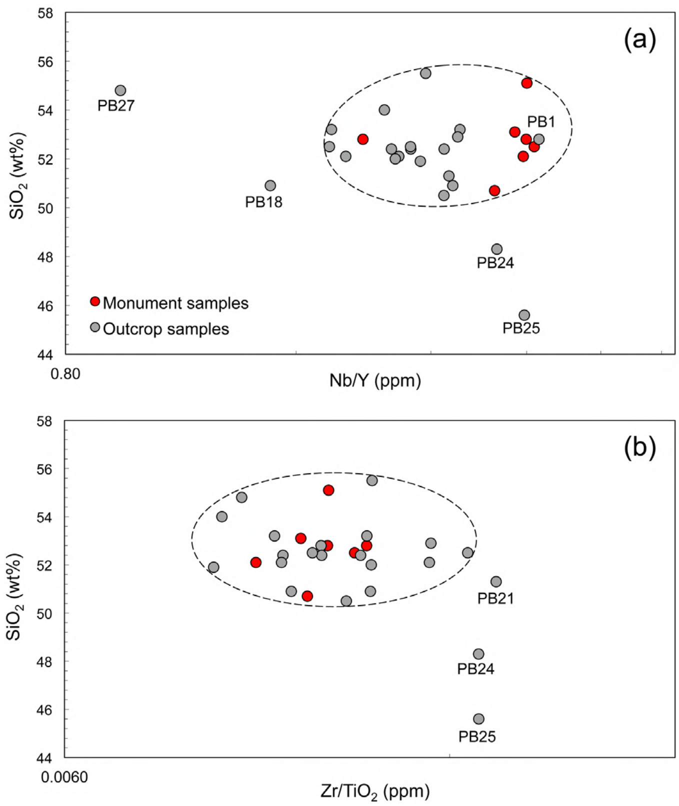

Fig. 16 - Binary diagrams of some immoble trace elements and major elements used to chemical discrimination of the volcanic samples from the monument and outcrops: (a) Nb/Y (ppm) vs. SiO_2 (wt%); (b) Zr/TiO_2 (ppm) vs. SiO_2 (wt%).

rise) that, subject to the cyclic processes of solubilization / recrystallization of hygroscopic phases, causes the decohesion of the rock, especially in the ashlar rows close to the ground.

The mortars used with structural function for bedding the stone ashlars have been correctly made, according to the conventional medieval construction methods, as confirmed by: 1) the absence of lime lumps, 2) the compositional homogeneity of the aggregate, 3) the more or less constant binder / aggregate ratio (~ 0.35-0.5). In fact, this latter result is in agreement with the ancient technical standards, which usually provide (in the case of structural-function mortars): from 2 to 3 parts of aggregate and 1 part of binder. Coherently with their technical function on the monument building, the plasters show a higher binder / aggregate (> 2 and more) with respect to the mortars and a lower size of aggregate fragments.

Mortars and plasters are unaffected by decay phenomena, especially the original ones, where it sporadically occurs. Alteration of the mortars generally is displayed with the occurrence of black crusts, exfoliation, and detachments. The newly formed minerals belong to the clay group and sulphates, in different associations and amounts. Gypsum is the only sulphate determined in the altered mortars. Its formation is due to the sulphation of carbonate phases, original components of the mortar binders. Newly formed gypsum can occur in different forms of alteration affecting the mortars (crusts, exfoliation, etc.)

CONCLUSIONS

The Basilica of Saccargia was built using in bychromy greyish-black local volcanites and whitish sedimentary stones (arenaceous limestones and marls).

The volcanic rocks belong to the Sardinian Plio-Pleistocenic volcanism and, according to the TAS diagram (Le Maitre *et alii*, 2002); they mainly are basaltic trachy-andesites. On the base of geochemical and mineral-petrographic studies, the sampling sites of most of the volcanic rocks used for the monument come from outcrops located near to the Basilica (500 m north), in locality *P. De Coloru* (Codrongianos, SS), and minor from the outcrops of the Ploaghe (SS) area in the following sites: *Su Trialzu*, *Mount Meddaris*, *Planu e Filighe* located at 3.8, 5.3, 7.2 km, respectively, from the Basilica (see Fig. 4). The Basilica construction, therefore, implied the supply from different areas not so far away from the monument. Moreover, taking into account the absence of any ancient basalt quarry in these areas, the mediaeval constructors possibly used blocks falling from the edge of the volcanic outcrops on the adjoining steep slope, and/or erratic stone boulders.

Physical results point out that the volcanic lithologies, used for the construction, have good mechanical strength (especially the massive facies, with porosity < 15% and point load strength > 5.5 MPa). In agreement with chemical, mineralogical and petrographic features, the basaltic rocks of the monument have a stable structure, narrowly susceptible to the attacks of the alteration processes. Minor physical decay (fractures, cracking close to the edges of ashlars) can be observed, due to the absence of bedding mortars under/between the ashlars and/or the presence of cement material mortars, the latter used in recent (last century) restore interventions.

The monument sedimentary stones come from *Florinas-Codrongianos* area. The presence of several limestone and marl facies, with variable volumetric amount of the intraclasts, as construction materials as well as in the outcrop, suggests the supply of raw material come from different points of extraction or from a single point in which there is a complete stratigraphy of outcropping lithologies. As in this area a complete stratigraphy is absent, the idea of different points of extraction is more likely, even through the use of erratic boulders. Indeed, marls and limestones crop out at elevations ranging from 350 to 450 MASL, in geomorphologic structures as cliffs and outliers, subjected to landslide gravity processes with the fall and the overthrow of stone blocks in the underlying valleys.

The sedimentary rocks show poor resistances to the weathering attacks. Both investigated limestones and marls are affected by evident physical decay and chemical alteration. The latter generally produces erosion on the ashlar surface, locally making disaggregation and detachment of material, generating retraction of the original ashlar surface. The artistic elements of Basilica show decay products due to the loss of the decorative shape, increasing the high specific surface area affected by weathering processes. Due to their different textural and micro-structural features, limestones and marls locally show different physical-mechanical behaviours as function on their compositional variability, cementing degree and porosity.

The homogeneous arenaceous limestone, regardless of porosity, generally shows greater mechanical strength than the more heterogeneous detritic organogenic facies. As concerns the alteration processes, somewhere the porous limestones of monument show dissolution processes of carbonate cement.

Marls show a wide variability of the mechanical strength as function of the decay degree. The less altered samples generally show greater values than the unaltered limestones. However, due to their mud-supported matrix and greater amount of arenaceous fraction with clay minerals, they frequently show major physical decay and minor chemical alteration: physical decay mainly occurs as the typical exfoliation, especially in the sites where major is the water circulation (*i.e.,* wash-out, capillary rise). Indeed, the cyclic mechanisms of hydration/dehydration of hygroscopic phases (*i.e.,* phyllosilicates) causes the inner decohesion of the rock matrix.

In agreement with Scano the ashlars or decorative elements of Basilica realised with marl (*e.g.,* capital and column of the portico) frequently showed over time a significant physical decay, thus requiring the replacement of the stone.

The squared stone ashlars were placed using aerial lime bedding mortars. The aggregate consists of quartz-feldspar sand that provides any compositional analogue with geological formation of *Superior* and *Inferior Sands (Ss, Si)* outcropping in *Florinas* area. The constructors extracted the raw materials for the mortars in this area. Due to the carbonate binder, the mortars and plasters occasionally show dissolution and sulphation processes with loss of material or formation of gypsum-crusts on the stone surface. In some cases, the decohesion or the absence of mortars between the ashlars produces physical-mechanical decay (fractures, cracking, especially in the sedimentary rocks) with consequent static problems in the walls of Basilica.

Acknowledgements

This research was funded by the "Regione Autonoma della Sardegna" within the research project entitled: "Romanesque and territory. The construction materials of the of Judicial Sardinia churches: new approaches for the enhancement, conservation and restoration", L.R. 7/2007, Scientific Coordinator: Stefano Columbu.

XRPD analyses were performed at the *Laboratorio di Didattica e Ricerca del Colle di Bonaria*, Via Ravenna snc, Cagliari (Italy). The Authors wish to thank the scientific coordinator of the Lab, Prof. Paola Meloni, of the *Dipartimento di Ingegneria Meccanica, Chimica e dei Materiali,* Università di Cagliari.

REFERENCES

Advokaat E.L., Van Hinsbergen D.J.J., Maffione M., Langereis C.G., Vissers R.L.M., Cherchi A., Schroeder R., Madani H. & Columbu S. (2014) - *Eocene rotation of Sardinia, and the paleogeography of the western Mediterranean region*. Earth and Planetary Science Letters, **401**, 183-195.

Assorgia A., Barca S. & Spano C. (1997) - *Lineamenti stratigrafici, tettonici e magmatici del terziario della sardegna. Libro guida La "Fossa Sarda" nell'ambito dell'evoluzione geodinamica cenozoica*, pp 13-25.

Antonelli F., Columbu S., De Vos Raaijmakers M. & Andreoli M. (2014a) - *An archaeometric contribution to the study of ancient millstones from the Mulargia area (Sardinia, Italy) through new analytical data on volcanic raw material and archaeological items from Hellenistic and Roman North Africa*. Journal of Archaeological Science, **50**, 243-261.

Antonelli F., Columbu S., Lezzerini M. & Miriello D. (2014b) - *Petrographic characterization and provenance determination of the white marbles used in the Roman sculptures of Forum Sempronii (Fossombrone, Marche, Italy).* Applied Physics A, **115**, 1033-1040.

Beccaluva L., Deriu M. & Macciotta G. (1981) - *Carta geopetrografica del vulcanismo plio-pleistocenico della Sardegna nord-occidentale.* Litografia Artistica Cartografica, Firenze.

Beccaluva L., Civetta L., Macciotta G. & Ricci C.A. (1985) - *Geochronology in Sardinia: results and problems*. Rendiconti della Società Italiana di Mineralogia e Petrologia, **40**, 57-72.

Beccaluva L., Brotzu P., Macciotta G., Morbidelli L., Serri G. & Traversa G. (1989) - *Cainozoic tectono-magmatic evolution and inferred mantle sources in the Sardo-Tyrrenian area*, in: Boriani, A., Bonafede, M., Piccardo, G.B., Vai, G.B. (Eds.), The lithosphere in Italy. Advances in Earth Science Research. Atti Conv. Acc. Naz. Lincei, **80**, 229-248.

Beccaluva L., Macciotta G. & Venturelli G. (1975) - *Dati geochimici e petrografici sulle vulcaniti Plio-Quaternarie della Sardegna centro-occidentale.* Boll. Soc. Geol. It., **94**, 1437-1457.

Beccaluva L., Macciotta G. & Venturelli G. (1976) - *Le vulcaniti plio-quaternarie del Logudoro (Sardegna nord-occidentale).* Boll. Soc. Geol. It., **95** (1-2), 339-350, Roma.

Beccaluva L., Deriu M., Macciotta G., Savelli C. & Venturelli G. (1977) - *Geochronology and magmatic character of the Pliocene-Pleistocene volcanism in Sardinia*. Bull. Volcanol., **40**, 1-16.

Beccaluva L., Coltorti M., Galassi B., Macciotta G. & Siena F. (1994) - *The Cainozoic calcalkaline magmatism of the western mediterranean and its geodynamic significance.* Boll. di Geofisica Teorica e Applicata, **36**, 141-144, 293-308.

Beccaluva L., Bianchini G., Coltorti M., Perkins Wt., Siena F., Vaccaro C., Wilson M. (2001) *Multistage evolution of the European lithospheric mantle: new evi- dence from Sardinian peridotite xenoliths*. Contrib. Mineral. Petrol., **142**, 284-297.

Beccaluva L., Bianchini G., Coltorti M., Siena F. & Verde M. (2005a) - *Cenozoic Tectono- magmatic Evolution of the Central-western Mediterranean: Migration of an Arc- interarc Basin System and Variations in the Mode of Subduction*. In: Finetti, I. (Ed.), Elsevier Special Volume, "Crop Project - Deep Seismic Exploration of the Central Mediterranean and Italy", pp. 623-640.

Beccaluva L., Bianchini G., Bonadiman C., Coltorti M., Macciotta G., Siena F. & Vaccaro C. (2005b) - *Within-plate Cenozoic Volcanism and Lithospheric Mantle Evolution in the Western-central Mediterranean Area*. In: Finetti, I. (Ed.), Elsevier Special Volume, "Crop Project - Deep Seismic Exploration of the Central Mediterranean and Italy", pp. 641-664.

Beccaluva L., Bianchini G., Natali C. & Siena F. (2011) - *Geodynamic control on orogenic and anorogenic magmatic phases in Sardinia and Southern Spain: Inferences for the Cenozoic evolution of the western Mediterranean.* Lithos, **180-181**, 128-137.

Bertorino G., Franceschelli M., Marchi M., Luglié C. & Columbu S. (2002) - *Petrographic characterisation of polished stone axes from Neolithic Sardinia, archaeological implications*. Per. Mineral., **71**, 87-100.

Burrus J. (1984) - *Contribution to a geodynamic synthesis of the Provençal basin (N-W Mediterranean).* Marine Geology, **55**, 247-269.

Carmignani L., Oggiano G., Funedda A., Conti P. & Pasci S. (2015) - *Geological map of Sardinia (Italy) at scale 1:250.000*. Journal of maps 2015.

Cherchi A., Mancin N., Montadert L., Murru M., Putzu M.T., Schiavinotto F. & Verrubbi V. (2008) - *The stratigraphic response to the Oligo-Miocene extension in the western Mediterranean from observations on the Sardinia graben system (Italy).* Bulletin de la Societe Geologique de France, **179**, 267-287.

Cherchi A. & Montadert L. (1982a) - *Il sistema di rifting oligo-miocenico del Mediterraneo occidentale e sue conseguenze paleogeografiche sul terziario sardo*. Mem. Soc. Geol. It., **24**, 387-400.

Cherchi A. & Montadert L. (1982b) - *Oligo-Miocene rift of Sardinia and the early history of the western Medittanean basin.* Nature, **298**, 736-739.

Columbu S. (2017) - *Provenance and alteration of pyroclastic rocks from the Romanesque Churches of Logudoro (north Sardinia, Italy) using a petrographic and geochemical statistical approach.* Applied Physics A, Materials Science & Processing, DOI: 10.1007/s00339-017-0790-z

Columbu S. (2018) - *Petrographic and geochemical investigations on the volcanic rocks used in the Punic-Roman archaeological site of Nora (Sardinia, Italy).* Earth Environmental Sciences, in press.

Columbu S. & Verdiani G. (2014) - *Digital Survey and Material Analysis Strategies for Documenting, Monitoring and Study the Romanesque*

Churches in Sardinia, Italy. Lecture Notes in Computer Science, Springer, **8740**, 446-453.

Columbu S., Antonelli F., Lezzerini M., Miriello D., Adembri B. & Blanco A. (2014a) - *Provenance of marbles used in the Heliocaminus Baths of Hadrian's Villa (Tivoli, Italy)*. Journal of Archaeological Science, **49**, 332-342.

Columbu S., Antonelli F. & Sitzia F. (2018a) - *Origin of Roman worked stones from St. Saturno Christian Basilica (south Sardinia, Italy).* Mediterranean Archaeology and Archaeometry, in press.

Columbu S., Cruciani G., Fancello D., Franceschelli M. & Musumeci G. (2015b) - *Petrophysical properties of a granite-protomylonite-ultramylonite sequence: insight from the Mt. Grighini shear zone, central Sardinia, Italy.* European Journal of Mineralogy, **27**(4), 471-486.

Columbu S., Garau A.M., Macciotta G., Marchi M., Marini C., Carboni D., Ginesu S. & Corazza G. (2011) - *Manuale sui materiali lapidei vulcanici della Sardegna centrale e dei loro principali impieghi nel costruito*. Ghilarza: Iskra Edizioni.

Columbu S., Gioncada A., Lezzerini M. & Marchi M. (2014b) - *Hydric dilatation of ignimbritic stones used in the church of Santa Maria di Otti (Oschiri, northern Sardinia, Italy).* Ital. J. Geosci., **133**, 149-160.

Columbu S., Lisci C., Sitzia F. & Buccellato G. (2017a) - *Physical-mechanical consolidation and protection of Miocenic limestone used on Mediterranean historical monuments: the case study of Pietra Cantone (southern Sardinia, Italy).* Environmental Earth Sciences, **76**(4), 148. DOI: 10.1007/s12665-017-6455-6

Columbu S., Marchi M., Martorelli R., Palomba M., Pinna F., Sitzia F., Tanzini L. & Virdis A. (2015b) - *Romanesque and Territory. The construction materials of Sardinian Medieval churches: new approaches to the valorisation, conservation and restoration.* In: Börner, W., Uhlirz, S. (Eds.), Proceedings of 16th International Conference on Cultural Heritage and New Technologies 2011 (CHNT16), Wien. Museen der Stadt Wien - Stadtarchäologie Ed., vol. 1, part 3, pp. 1-15.

Columbu S., Piras G., Sitzia F., Pagnotta S., Raneri S., Legnaioli S., Palleschi V., Lezzerini M. & Giamello M. (2018b) - *Petrographic and mineralogical characterization of volcanic rocks and surface-depositions on Romanesque monuments.* Mediterranean Archaeology and Archaeometry, in press.

Columbu S., Sitzia F. & Ennas G. (2017a) - *The ancient pozzolanic mortars and concretes of Heliocaminus baths in Hadrian's Villa (Tivoli, Italy).* Archaeol Anthropol Sci, **9**(4), 523-553.

Columbu S., Sitzia F. & Verdiani G. (2015a) - *Contribution of petrophysical analysis and 3D digital survey in the archaeometric investigations of the Emperor Hadrian's Baths (Tivoli, Italy).* Rend. Fis. Acc. Lincei, **26**, 455-474.

Columbu S. & Garau A.M. (2017) - *Mineralogical, petrographic and chemical analysis of geomaterials used in the mortars of Roman Nora theatre (south Sardinia, Italy).* Ital. J. Geosci., **136**(2), 238-262.

Coroneo R. (1993) - *Architettura romanica dalla metà del Mille al primo '300*. Ilisso, Nuoro.

Coroneo R. & Columbu S. (2010) - *St. Antioco di Bisarcio (Ozieri): La cattedrale romanica e i materiali costruttivi.* Archeoarte, **1**, 145-173.

Coulon C. (1977) - *Le volcanisme calco-alcalin cenozoique de Sardaigne, Italie.* Unpublished master's thesis, Univesité St. Jerome, Marseille.

Criss J.W. (1977) - *NRLXRF: a fortran program for X-Ray fluorescence analisys*. Cosmic, Athens, Georgia.

Cross W., Iddings J.P., Pirsson L.V. & Washington H.S. (1903) - *Quantitative classification of igneous rocks*. University of Chicago Press.

Dostal J., Coulon C. & Dupuy C. (1982) - *Cainozoic andesitic rock of Sardinia (Italy).* In: Thorpe, R.S. (Ed.), Andesites: orogenic andesites and related rocks (pp. 353-370). Chichester: J. Wiley & Sons.

Folk R.L. (1968) - *Petrology of sedimentary rocks*. Texas: Hemphill's Austin.

Gasperini D., Blichert-Toft J., Bosch D., Del Moro A., Macera P., Télouk P. & Albarède F. (2000) - *Evidence from Sardinian basalt geochemistry for recycling of plume heads into the Earth's mantle*. *Nature*, **408**, 701-704.

Gasperini D., Blichert-Toft J., Bosch D., Del Moro A., Macera P. & Albarède F. (2002) - *Upwelling of deep mantle material through a plate window: Evidence from the geochemistry of Italian basaltic volcanics*. Journal of Geophysical Research, **107**, B2367, http://dx.doi.org/10.1029/2001JB000418.

Gizzi S. (2007) - *SS. Trinità di Saccargia restauri 1891-1897*. Gangemi. Roma.

International Society For Rock Mechanics (1972) - *Suggest method for determining the point load strength index*. Committee on Field Tests, **1**, 8-12.

International Society For Rock Mechanics (1985) - *Suggest Method for determining the point load strength index ISRM. Commission for Testing Methods, Working Group on Revision of the Point Load Test Methods*. Int. J. Rock Mech. Min. Sci. and Geomech., **33**, 51-60.

Johannsen A.A. (1973) - *Descriptive Petrography of the Igneous Rocks. Volume 1, Introduction, Textures, Classifications, and Glossary*. The University of Chicago Press, Chicago.

Kuno H. (1968) - *Differentiation of basalt magma*. In: the Poldervaart treatise on rocks of basaltic composition. Ed. H. Hess, A. Poldervaart, Vol. II, Wiley & Sons, New York, pp. 623-688.

Le Bas M.J., Le Maitre R.W., Streckeisen A. & Zanettin B. (1986) - *A chemical classification of volcanic rocks based on the total alkali silica diagram*. Journ.Petrol., **27**, 745-750.

Le Maitre R.W, Streckeisen A., Zanettin B., Le Bas MJ., Bonin B., Bateman P., Bellieni G., Dudek A., Efremova S., Keller J., Lamere J., Sabine P.A., Schmid R., Sorensen H. & Woolley A.R. (2002) - *Igneous Rocks: A Classification and Glossary of Terms. Recommendations of the International Union of Geological Sciences, Subcommission of the Systematics of Igneous Rock*s. Cambridge University Press, Cambridge.

Lezzerini M., Antonelli F., Columbu S., Gadducci R., Marradi A., Miriello D., Parodi L., Secchiari L. & Lazzeri A. (2016) - *The Documentation and Conservation of the Cultural Heritage: 3D Laser Scanning and Gis Techniques for Thematic Mapping of the Stonework of the Façade of St. Nicholas Church (Pisa, Italy).* International Journal of Architectural Heritage: Conservation, Analysis, and Restoration, **10**(1), 9-19.

Lezzerini M., Pagnotta S., Raneri S., Legnaioli S., Palleschi V., Columbu S., Neri N.F. & Mazzoleni P. (2018) - *Examining the reactivity of volcanic ash in ancient mortars by using a micro-chemical approach*. Mediterranean archaeology and archaeometry, in press.

Lustrino M., Morra V., Melluso L., Brotzu P., D'amelio F., Fedele L., Lonis R., Franciosi L. & Petteruti Lieberckneckt A.M. (2004). *The Cenozoic igneous activity in Sardinia*. Per. Mineral., **73**, 105-134.

Lustrino M., Melluso L., Morra V. (2000) - *The role of continental crust and lithospheric mantle in the genesis of Plio-Pleistocene volcanic rock from Sardinia (Italy)*. Earth and Planetary Science Letters, **180**, 259-270.

Lustrino M., Brotzu P., Lonis R., Melluso L., Morra V. (2004) - *European subcontinental mantle as revealed by Neogene volcanic rocks and mantle xenoliths of Sardinia*. Field trip guide, IGC Florence 2004.

Lustrino M. & Wilson M. (2007) - *The circum-Mediterranean anorogenic Cenozoic igneous province*. Earth-Science Reviews, **81**, 1-65.

Lustrino M., Morra V., Fedele L. & Franciosi L. (2009) - *Beginning of the Apennine subduction system in central western Mediterranean: constraints from Cenozoic "orogenic"magmatic activity of Sardinia, Italy*. Tectonics, **28**, TC5016.

Lustrino M., Duggen S. & Rosenberg C.L. (2011) - *The Central-Western Mediterranean: anomalous igneous activity in an anomalous collisional tectonic setting*. Earth-Science Reviews, **104**, 1-40.

Lustrino M., Fedele L., Melluso L., Morra V., Ronga F., Geldmacher J., Duggen S., Agostini S., Cucciniello C., Franciosi L. & Meisel T. (2013) - *Origin and evolution of Cenozoic magmatism of Sardinia (Italy). A combined isotopic (Sr-Nd-Pb-O-Hf-Os) and petrological view* Lithos, **180-181**, 138-158.

Macciotta G., Bertorino G., Caredda A., Columbu S., Coroneo R., Franceschelli M., Marchi M. & Rescic S. (2001) - *The S.Antioco of Bisarcio Basilica (NE Sardinia, Italy): water-rock interaction in ignimbrite monument decay.* In: Cidu (Ed.), Water-Rock Interaction, Lisse: Swets & Zeitlinger, pp. 415-418.

Mazzei R. & Oggiano G. (1990) - *Messa in evidenza di due cicli sedimentari nel miocene dell'area di Florinas (Sardegna settentrionale)*. Atti Società Toscana di Scienze Naturali. Mem. Serie A, **97**, 119-147.

Melis S. & Columbu S. (2000) - *Matériaux de construction en époque romaine et aves les anciennes carrières: l'exemple du théâtre de Nora (Sardaigne SO, Italie)*. In: Lorenz, J., Tardy, D., Coulon, G. (Eds.), La pierre dans la ville antique et médiévale. Analyse méthodologie et apports, Argentoun sur Creuse. Saint-Marcel: Musée d'Argentomagus.

Miriello D., Antonelli F., Apollaro C., Bloise A., Bruno N., Catalano E., Columbu S., Crisci G.M., De Luca R., Lezzerini M., Mancus S. & La Marca A. (2015) - *New data about the ancient mortars from the archaeological site of Kyme (Turkey): compositional characterization*. Per. Min., **84**, 3A, 497-517.

Palmstrom A. (1995) - *RMi-a rock mass characterization system for rock engineering purposes*. PhD. thesis, University of Oslo, Norway, 430 pp.

Peccerillo A. (2005) - *Plio-Quaternary Volcanism in Italy.* Petrology, Geochemistry, Geodynamics. Springer, Heidelberg.

Peccerillo A. & Frezzotti M.L. (2015) - *Magmatism, mantle evolution and geodynamics at the converging plate margins of Italy*. JCS, **172**, 407-427.

Piromallo C. & Morelli A. (2003) - *P-wave tomography of the mantle under the Alpine- Mediterranean area*. Journal of Geophysical Research, **108**, 1-23.

Recommendations Nor.Ma.L. 3/80 (1980) - *Stone materials: Sampling*. Roma: CNR - ICR.

Savelli C. (1988) - *Late Oligocene to recent episodes of magmatism in and around the Tyrrhenian Sea: implication for the processes of opening in a young inter-arc basin of intra orogenic (Mediterranean) type*. Tectonophysics, **146**(1-4), 163-181.

Sechi A.L. (1992) - *Ritrovare Saccargia, Documento grafico storico della basilica romanica "La SS. Trinità"*. Dattena, Cagliari.

Serra R. (1988) - *Sardegna Romanica*. Jaka book, Milano.

Shand S.J. (1951) - *Eruptive rocks; their genesis, composition, classification, and their relation to ore-deposits, with a chapter on meteorites*. 4th ed, Wiley, New York.

Spakman W. (1990) - *Tomographic images of the upper mantle below central Europe and the Mediterranean*. Terra Nova, **2**, 542-553.

Streckeisen A.L. (1974) - *Classification and Nomenclature of Plutonic Rocks. Recommendations of the IUGS Subcommission on the Systematics of Igneous Rocks*. Geologische Rundschau, Internationale Zeitschrift für Geologie, Stoccarda, 773-785.

Thornton C.P. & Tuttle O.F. (1960) - *Chemistry of igneous rocks, I. Differentiation index*. American Journal of Science, **258**, 664-684.

Verdiani G. & Columbu S. (2010) - *E. Stone, an archive for the Sardinia monumental witnesses*. In: Third International Conference, EuroMed 2010, Lemessos, Cyprus, November 8-13, 2010. Book Chapter in 'Lecture Notes in Computer Science' (LNCS), vol. 6436/2010. Springer, Berlin-Heidelberg, pp. 356-372.

Vivanet F. (1902) - *Cagliari antica, medievale e moderna*. Valdès, Cagliari.

Manuscript received 12 August 2017; accepted 27 February 2018; published 05 March 2018
editorial responsibility and handling by A. Renzulli